COMBINED SOURCE-CHANNEL CODING FOR A POWER AND BANDWIDTH CONSTRAINED NOISY CHANNEL

A Thesis

by

NOUMAN SAEED RAJA

Submitted to the Office of Graduate Studies of
Texas A&M University
in partial fulfillment of the requirements for the degree of

MASTER OF SCIENCE

December 2003

Major Subject: Electrical Engineering

COMBINED SOURCE-CHANNEL CODING FOR A POWER AND BANDWIDTH CONSTRAINED NOISY CHANNEL

A Thesis

by

NOUMAN SAEED RAJA

Submitted to the Office of Graduate Studies of
Texas A&M University
in partial fulfillment of the requirements for the degree of

MASTER OF SCIENCE

Approved as to style and content by:

Zixiang Xiong (Chair of Committee)	Costas N. Georghiades (Member)
Andreas Klappenecker (Member)	Jose Silva-Martinez (Member)
Chanan Singh (Head of Department)	

December 2003

Major Subject: Electrical Engineering

ABSTRACT

Combined Source-Channel Coding for a Power and

Bandwidth Constrained Noisy Channel. (December 2003)

Nouman Saeed Raja, B.S, GIK Institute of Engineering Sciences & Technology

Chair of Advisory Committee: Dr. Zixiang Xiong

This thesis proposes a framework for combined source-channel coding under power and bandwidth constrained noisy channel. The framework is then applied to progressive image coding transmission using constant envelope M-ary Phase Shift Key (MPSK) signaling over an Additive White Gaussian Channel (AWGN) channel. First the framework for uncoded MPSK signaling is developed. Then, it's extended to include coded modulation using Trellis Coded Modulation (TCM) for MPSK signaling. Simulation results show that coded MPSK signaling performs 3.1 to 5.2 dB better than uncoded MPSK signaling depending on the constellation size. Finally, an adaptive TCM system is presented for practical implementation of the proposed scheme, which outperforms uncoded MPSK system over all signal to noise ratio (Es/No) ranges for various MPSK modulation formats.

In the second part of this thesis, the performance of the scheme is investigated from the channel capacity point of view. Using powerful channel codes like Turbo and Low Density Parity Check (LDPC) codes, the combined source-channel coding scheme is shown to be within 1 dB of the performance limit with MPSK channel signaling.

DEDICATION

This Thesis is dedicated with all my heart to:

My Parents, whose love, sacrifice and prayers made me reach this moment.

To my brother and sisters, for their support and encouragement throughout my life.

To my grandmother for her sincere support and prayers.

ACKNOWLEDGEMENTS

I would like to express my deepest gratitude to Dr. Zixiang Xiong for his guidance and encouragement. He has been a source of inspiration, throughout my graduate studies at Texas A&M University.

I would like to thanks Dr. Marc Fossorier, Department of Electrical Engineering, University of Hawaii, for his help and suggestions.

I extend my appreciation to Dr. Costas N. Georghiades, Dr. J. Silva-Martinez and Dr. A. Klappenecker for the time they dedicated to me.

I want to express my sincere gratitude to my colleagues in the Multimedia Laboratory, for sharing their insightful knowledge with me. I am especially grateful to Mr. Vivek Gullati and Mr. Hari Sankar for their many helpful suggestions and assistance. I also want to express my deep appreciation to my friends, Mr. Ahsan Ali and Mr. Asher Imam, for their help and support.

I would also like to acknowledge my professors at Texas A&M University; from whom I have learned so much.

Finally I would like to thank my family and friends who have always been a source of inspiration and motivation.

TABLE OF CONTENTS

Page

CHAPTER Page

LIST OF FIGURES

FIGURE Page

LIST OF TABLES

CHAPTER I

INTRODUCTION

A fundamental problem in the communication theory is that of achieving reliable transmission of data from one point to another. Shannon [1] showed that a channel has a limit on the maximum amount of information, called the *channel capacity* that can be transmitted over this channel without incurring any error. Subsequently, Shannon [2] showed that given a discrete, stationary and ergodic source and a single letter distortion measure there is a rate-distortion function that can be interpreted as the minimum information rate of the source for a given level of distortion. These results form the backbone of the two main branches of communication research: i.e., source coding and channel coding. In source coding, the aim is to represent the source with fewer bits by removing redundancy in the source. In essence, the aim is to approach the rate-distortion (R-D) bound as closely as possible. In channel coding the aim is to protect the source from the errors that are introduced by the channel. This goal is often achieved by the introduction of controlled redundancy. These requirements often lead to an engineering compromise, commonly referred to as joint source and channel coding (JSCC). This thesis presents a JSCC model for certain class of source and channel coders with a constraint on channel power and bandwidth.

The cost of using a power-constrained channel, such as the Additive White Gaussian Noise (AWGN) channel, is often described by the average energy transmitted per source symbol. For a given modulation signal constellation, the transmission rate is a design parameter that can be formulated to optimize the end-to-end quantization error of the system. A given transmission rate implies a particular number of bits transmitted per source symbol. These bits are generated by sending source coding bits through a channel code. An important problem is how to effectively allocate these bits between coding the

---

This thesis follows the style and format of *IEEE Transactions on Information Theory.*

source and providing protection against channel errors. This allocation is characterized by the choice of a channel code rate, which determines what fraction of the transmission rate is for source coding and what fraction is for channel coding. By introducing a bandwidth constraint, this degree of freedom becomes the choices of signal constellation in conjunction with both the channel code rate (resulting in coded-modulation) and the source code rate. Thus, there is a tradeoff between modulation, source coding, and channel coding. These components will be examined by jointly optimizing the transmission rate and the channel code rate for certain class of source and channel codes. The goal is to minimize the rate-distortion measure for image transmission over a bandwidth and power constrained noisy channel.

Sherwood and Zeger [3] used a combined source-channel scheme based on Said and Pearlman's Set Partitioning in Hierarchical Trees (SPIHT) source coding algorithm [4]. They utilized rate compatible punctured convolutional (RCPC) channel codes for image transmission over a binary symmetric channel (BSC). Since then, numerous authors [5]-[8] have worked on JSCC for scalable multimedia transmission over both BSC and packet erasure channels (PEC). M. Fossorier et al. [9] generalized the scheme of Sherwood and Zeger [3] from a discrete binary channel model to an analog binary channel by allowing to choose the average energy per transmitted bit in conjunction with both the source rate and the channel code rate under a power constraint. While this additional degree of freedom allows achieving higher overall Peak Signal to Noise Ratio (PSNR) values, it also results in either bandwidth reduction or expansion with respect to the underlying reference system, the latter being highly undesirable.

The embedded property of SPHIT source coder is also exploited to provide Unequal Error Protection (UEP) [10]-[13] by the use of different channel codes with codes of higher rates allocated to the tail of the source coder output. For example, in the results reported in [11], the rate 10/12, 11/12 and 12/12 codes provide very little error protection. Thus, a more efficient transmission scheme could be obtained with constellation expansion: coded modulation.

Forward Error Correction (FEC) coding is a practical technique for increasing the transmission efficiency of virtually all-digital communication channels. Efficiency applies to both power and bandwidth required to support a given information rate, or conversely to increase the information rate to be transmitted at a given bandwidth and power. G. Ungerboeck [14] showed that with Trellis Coded Modulation (TCM), it is possible to achieve Asymptotic Coding Gain (ACG) of as much as 6 dB in average energy per symbol (Es/No) within precisely the same signal spectral bandwidth, by doubling the signal constellation set for $M = 2^{k-1}$ to $M = 2^k$ using *Set Partitioning* coupled with rate (k-1)/k convolutional code. The main idea was to optimize the Euclidean space rather than dealing with Hamming distance. The set partitioning strategy maximizes the intra-subset Euclidean distance. The least significant bits are normally convolutionally encoded and most significant bits may be left uncoded. The coded bits are then mapped on to a point on the constellation. The code parameters are chosen with the help of an exhaustive computer search in order to maximize the minimum distance of coded sequences in Euclidean space. Because of the trellis constraints on the sequences of the signal points, this method is called Trellis Coded Modulation (TCM). This lead to an extensive research [15]-[16] in coding theory to find practical codes and their performance bounds. A. J. Viterbi et, al. [17] introduced bandwidth efficient Pragmatic Trellis Code which generates trellis codes for higher MPSK constellation by using an industrial standard rate 1/2 Trellis Code, at the loss of some performance compared to Ungerboeck codes. J. K. Wolf and E. Zehavi [18] extended Pragmatic Trellis codes to a wide range of high-rate punctured trellis codes for both PSK and QAM modulation.

In this thesis, the JSCC framework is designed for the SPHIT embedded image coder. The Es/No is chosen in conjunction with source coder and channel coder under the power constraint. Similarly, TCM is used in combination with the bandwidth constraint. The performance of TCM system saturates quickly as compared to uncoded modulation. So, some Es/No regions might exist where the performance of uncoded system is better. Using Punctured, Pragmatic and P^2 TCM codes, an adaptive TCM system is designed that is optimal for variable rate and modulation formats. TCM coders

are used primarily as their existing theoretical performance bounds can be computed analytically. Thus, simulations can be used to match the exact performance of TCM coders and the JSCC system.

Recently, C. Berrou and A. Glavienux introduced Turbo codes [19] and D. MacKay and R. Neal [20] showed that Low-Density Parity Check (LDPC) codes proposed by R. Gallager [21] are within one dB of Shannon's capacity limit. These random codes however provide loose theoretical bounds as compared to TCM codes. Simulation results using Turbo and LDPC codes are also presented in this study. Using these codes, the Turbo and LDPC based JSCC system has a *gap* of 1.2 dB and 0.92 dB respectively, from the Capacity-Achieving SNR (SNR Gap) value for QPSK channel.

This thesis is organized as follows. In chapter II, we review SPHIT embedded coder and present the JSCC framework using SPHIT coder under power and bandwidth constrained noisy channel. The JSSC system is then formulated for generic uncoded and coded signaling formats. In chapter III, we review the theory of MPSK modulation and coded modulation techniques (e.g., TCM codes). The framework is then applied to MPSK signaling. Theoretical and simulation results for both uncoded and coded cases are presented followed by the design of an adaptive TCM system. The input constrained capacity for AWGN Channel is considered in chapter IV. Results are presented for MPSK modulation. Also, the theory and design of Turbo and LPDC codes are explained for the case of coded modulation. The results of applying these codes to the JSCC scheme are also presented. Finally, we present the conclusions in chapter V.

CHAPTER II

JSCC FRAMEWORK

2.1 Introduction

The separation principle of Shannon [1] showed that source coding and channel coding could be optimized individually and then operated in a cascaded system without any sacrifice in optimality. Traditionally, source coders are designed for an ideal noiseless channel while channel coders are designed to minimize the average probability of decoding error irrespective of the actual source, and the resulting encoders and decoders are cascaded. However, Shannon's separation principle is valid only for asymptotic conditions like infinite block length and memoryless channel. Thus, under practical delay and storage constraints, independent design of source and channel coders is not optimal. This motivates a coupled design of source code and channel code. One approach is to use a combined source-channel coder to replace the cascade of a source coder and a channel coder. The complexity of the joint optimization of a combined source-channel coder, however, quickly becomes prohibitive for systems of practical size. Thus, not only does the traditional separation approach require infinite complexity for optimality, but also a completely coupled design is also infeasible. This thesis therefore, presents a low complexity technique, which increases the performance of cascaded systems by introducing some amount of coupling between the source coder and the channel coder. In particular, source/channel rate (bit) allocation is studied for embedded source coders under a power and bandwidth constrained noisy channel. A progressive image encoder based on SPIHT algorithm is used and a JSCC framework that minimizes the distortion under power and bandwidth constraints for the channel is presented.

2.2 SPHIT Codec

The SPIHT coder by Said and Pearlman [4] is a popular wavelet-based image coder. It uses octave-band filter-banks in the subband decomposition of the image and takes the advantage of the fact that the variance of the coefficients decreases from the lowest to the highest bands in the subband pyramid. This scheme is an improvement of the embedded zero tree coding algorithm or the EZW algorithm by Shapiro [22]. Both schemes produce an embedded bit stream, which means that the decoding can be stopped at any point and the image can be decoded to some level of accuracy. The difference between the SPIHT and EZW algorithms is that the SPIHT algorithm provides better performance. Also, the EZW algorithm requires arithmetic encoding of the bit stream for good compression, whereas the SPIHT algorithm can perform reasonably well even without arithmetic coding. This is so because the subset partitioning is very effective in the SPIHT algorithm and the resulting significance information is very compact.

The crux of the SPIHT algorithm lies in ordering the subband coefficients according to their magnitude and transmitting the most significant bits of the significant coefficients first. The algorithm is based on three concepts:

- Partial ordering of the transformed image coefficients by magnitude, with transmission of order by a subset-partitioning algorithm that is duplicated at the decoder end.
- Ordered bit plane transmission of refinement bits.
- Exploitation of self-similarity of the wavelet coefficients across different scales.

The wavelet coefficients are expected to be better magnitude ordered if we move down the pyramid following the same spatial orientation. For example, large low-activity areas are expected to be identified in the highest levels of the pyramid and they are replicated at the lower levels at the same spatial locations. An example of the

dependencies of the coefficients across different scales is shown in Fig. 1. In the Figure, the outermost rectangle represents the 2-D frequency plane of the image. The first filtering operation produces the first four (largest) quadrants in the Fig. 1. Since an image is a 2-D signal, one might use different filters for the horizontal and the vertical directions. If we classify the filters into the low-pass and the high-pass filters, then we have four possible frequency bands corresponding to the four possible combinations of the filters and the directions. Hence, the LL-band (I quadrant in the Fig. 1) corresponds to filtering the image in both directions using a low-pass filter; the II quadrant corresponds to the low-high band and so on.

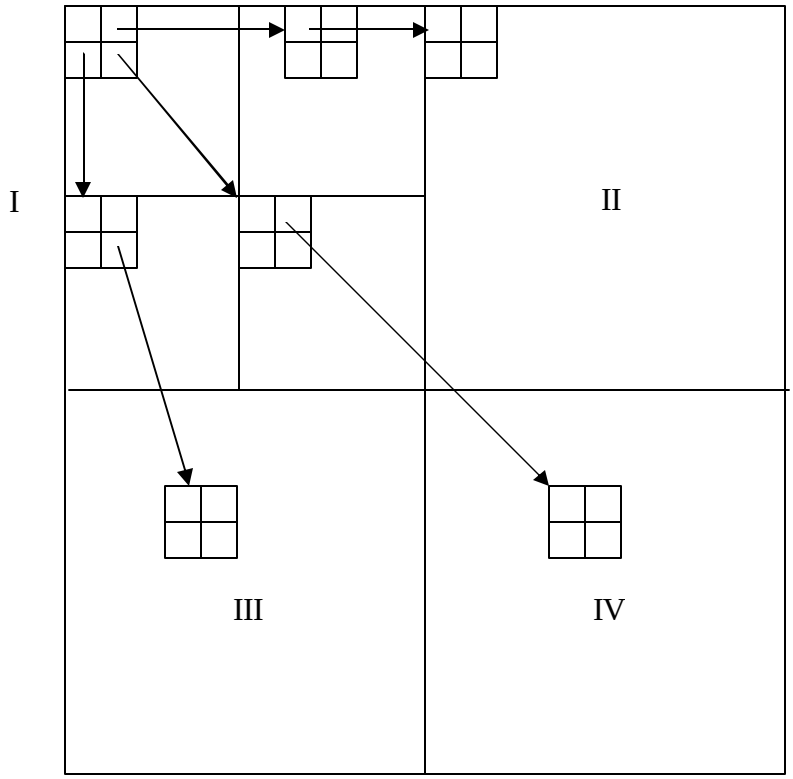

Fig. 1. Examples of parent-offspring dependencies in the spatial orientation tree

The algorithm can be basically divided into the *sorting pass* and the *refinement pass*. The sorting pass uses what is known as the spatial orientation tree. This tree is built based on the observation that there is a spatial self-similarity between the subbands (see Fig. 1). Each node in the tree corresponds to a pixel and is identified by the pixel coordinate. Its direct descendants correspond to pixels of the same spatial orientation in the next finer level of the pyramid. In Fig. 1, the arrows are oriented from the parent to its four off-springs. Parts of the spatial orientation tree are used as the partitioning subsets in the sorting algorithm. The sorting pass orders the coefficients according to their significance, which is judged by the amount of reduction in distortion that can be gained upon receiving a coefficient at the decoder.

The refinement pass transmits the most significant bit of all the coefficients contained in the list of significant pixels, except those included in the previous sorting pass. A large fraction of the *bit-budget* is spent on the sorting pass and it is there that the sophisticated coding methods are needed; hence the quantizer can be kept simple (e.g. a scalar quantizer).

The SPIHT algorithm allocates the available bit-budget between encoding the treemap (which indicates the location of the significant coefficients) and the significance information itself (which indicates the energy of the coefficients). It allows for precise rate control and affordable computational complexity. The SPIHT quantizer is reported to surpass other coding techniques such as JPEG, EZW, etc. It offers a variety of good characteristics. These characteristics include:

- Good image quality with a high Peak Signal to Noise Ratio (PSNR).
- Fast coding and decoding.
- A fully progressive bit-stream.
- Can be used for lossless compression.
- Ability to code for exact bit rate or PSNR.

The main advantage of SPIHT is that it is fully progressive, meaning that we do not need the whole file to see the image. The image's PSNR will be directly related to the amount of the bits received from the transmitter. Fig. 2 shows the rate-distortion curve of Lena image transmitted in terms of PSNR. As the percentage of bit decoded correctly increases, the distortion decreases or PSNR of the image increases. This effect is shown in Fig. 3.

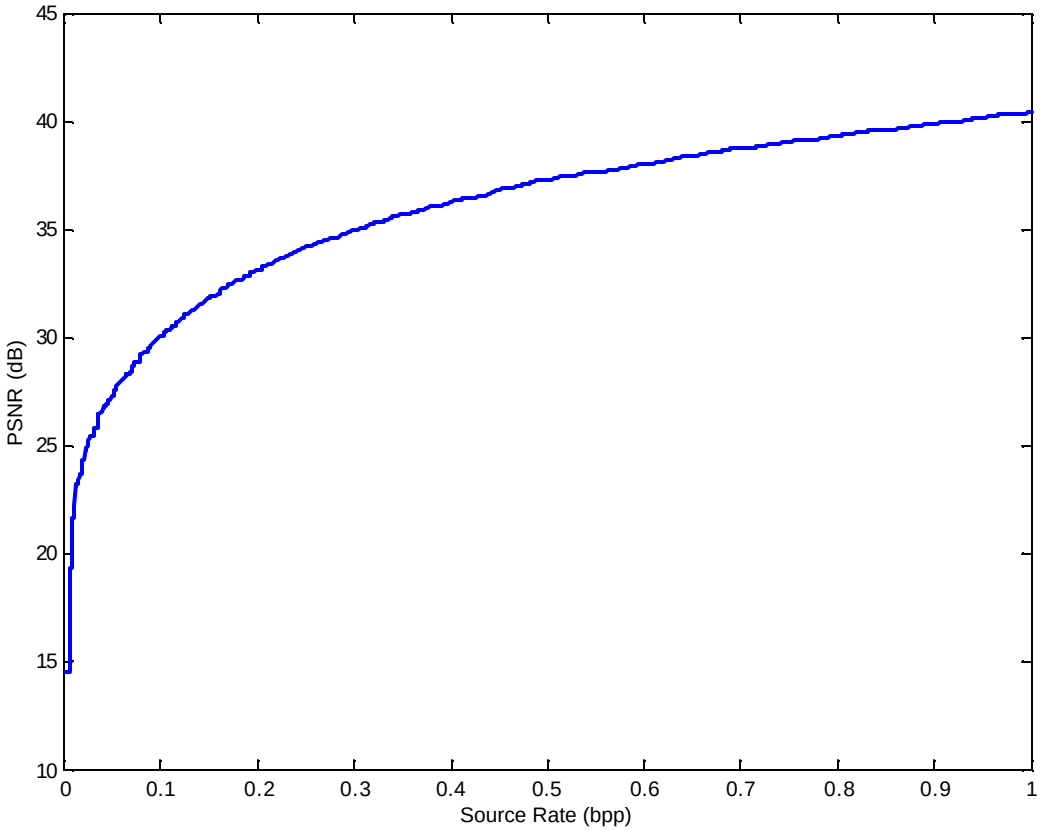

Fig. 2. Rate-PSNR (distortion) curve of Lena image

(0.10 bpp)

(0.25 bpp)

(0.50 bpp)

(0.75 bpp)

(1.0 bpp)

(original)

Fig. 3. Progressive decoding of Lena image

2.3 Framework

Consider a JSCC system employing a SPHIT image source emitting bits at the rate r_s (measured in bits per source sample). The quality of sampled and encoded analog source can be characterized by distortion D as a function of its rate r_s (measured in bits per source sample). It is assumed that D is monotonically non-increasing function of r_s.

In this case, D measures the mean-square quantization error of decompressed image in terms of the number of bits per pixel present in the compressed version of the image. As the source is progressively compressed, decoding stops if a single error occurs, thus the average Rate distortion for an N-bit source at a given P_b (E_b/N_0) can be calculated as

$$D_{avg}(E_b/N_0) = D(N)[1 - P_b(E_b/N_0)]^N + \sum_{i=0}^{N-1} D(i)[1 - P_b(E_b/N_0)]^i P_b(E_b/N_0) \qquad (1)$$

If R constellation signals per source sample are transmitted over the channel, the average energy E_s per transmitted signal must satisfy following equation under the power constraint.

$$R \cdot E_s \leq P \qquad (2)$$

The bandwidth constraint implies signal duration per channel use of at least $1/R_0$ second, so that $R=R_0$ implies following equation if both the maximum available power and maximum available bandwidth are used.

$$E_s = \frac{P}{R_0} \tag{3}$$

If channel code with rate r_c (measured in source bits per channel use) is used for error correction, the number of bits per source sample available for source coding is:

$$r_s = R_0 \cdot r_c \tag{4}$$

To each constellation $\{S_i\}$ used for transmission over the channel considered is associated its capacity $C_i\,(E_s / N_0)$. Shannon's channel coding theorem shows that if

$$r_c < C\left(E_s / N_0\right) \tag{5}$$

Then, r_s bits per source sample can be transmitted with arbitrarily small probability of error and Shannon's separation principle shows that the distortion, corresponding to rate r_s can be achieved.

Since, D is assumed to be non-increasing function of r_s this simply suggests *selecting the signal constellation, which achieves the largest capacity value under the power and bandwidth constraints*, although it assumes unboundedly long block lengths.

2.4 Application to an Arbitrary Modulation Format for an AWGN Channel

In this section, the following practical problem based on the progressive image coders SPHIT is considered. For given AWGN channel with zero-mean and variance $N_0/2$, and both an average power constraint and bandwidth constraint, what is the minimum achievable average mean-squared error (MSE) of transmitted image using Arbitrary Modulation Signaling (AMS) for both coded and uncoded case?

2.4.1 Uncoded M-ary AMS Signaling

The SPIHT image coder is used in conjunction with 2^k–*AMS* signaling. The corresponding uniform average bit error probability is computed and given as $P_b(k)$. For an M =512 × 512 image compressed at rate of r_s bpp and 2^k–*AMS* signaling, $kb_0 = M\, r_s$ bits are transmitted over the AWGN with b_0 symbols. Due to the embedded nature of the source coder, the average MSE can be expressed as

$$D(1,k) = D(r_s)(1-P_b(k))^{kb_0} + \sum_{i=0}^{kb_0-1} D(r_s i / kb_0)(1-P_b(k))^i P_b(k) \qquad (6)$$

where $D(r_s)$ represents the distortion of the image compressed at rate of r bpp.

The corresponding source code rate is $r_s = kb_0 / M$. Since, $D(kb_o / M)$ decreases as k increases while $P_b(k)$ increases as k increases, this implies that for given value E_s / N_0 the optimum choice of k corresponds to the MSE

$$D_{unc,\min}(E_s / N_0) = \underbrace{\min}_{k}\{D(1,k)\} \qquad (7)$$

Intuitively, this choice is justified by the fact that as the channel conditions improves (i.e. E_s/N_0 increases); larger constellation (i.e. larger value of k) can be chosen which results in larger value of r_s and lower MSE.

Improved average MSE can be obtained if channel coding is combined with the modulation, resulting in coded modulation. The following section illustrates how to obtain such gain.

2.4.2 Coded M-ary AMS Signaling

Assume rate r_c/k channel code is used to transmit an M = 512 × 512 image compressed at rate of r_s bpp with 2^k–*AMS* signaling, so that $r_c b_0 = M\ r_s$. If the corresponding bit error probability is approximated as $P_b(k)$. Then, corresponding average MSE becomes

$$D(1,k) = D(r_s)(1-P_b(k))^{r_c b_0} + \sum_{i=0}^{r_c b_0 - 1} D(r_s i / r_c b_0)(1-P_b(k))^i P_b(k) \qquad (8)$$

We optimize,

$$D_{cod,\min}(E_s / N_0) = \underbrace{\min}_{r_c,k}\{D(r_c,k)\} \qquad (9)$$

In terms of PSNR, it becomes,

$$PSNR = 10 * \log_{10}\left(\frac{255^2}{D_{opt}(E_s / N_0)}\right) \qquad (10)$$

Now depending on the channel conditions we will optimize both the code rate and modulation format that gives minimum distortion (maximum PSNR).

CHAPTER III

M-ary PSK MODULATION

In this chapter, the JSCC scheme presented in the previous chapter is applied to MPSK modulation. Followed by the extension of this scheme to coded modulation techniques for MPSK e.g. TCM codes, a practical TCM system optimal for variable rate and signal constellation is presented. Forward Error Correcting (FEC) coding like TCM is a practical technique for increasing the transmission efficiency of virtually all-digital communication channels. Efficiency applies to both the power & the bandwidth required to support a given information rate, or conversely to increase the information rate to be transmitted at a given bandwidth and power.

3.1 Phase Shift Keying

Phase shift keying (PSK) is a modulation scheme where the source information is contained in the phase of the transmitted carrier. The set of waveforms for an M (2^k)-ary PSK signaling is described by

$$x_m(t) = \begin{cases} \sqrt{\frac{2E_s}{T}}\cos(w_o t - 2pm/M)\,;\ 0 \le t \le T\,; \\ 0 \qquad\qquad\qquad\qquad\qquad\qquad ;\ \text{Otherwise} \end{cases} \tag{11}$$

The PSK signal set is an equal energy set and the constellation is contained on a circle of radius $\sqrt{E_s}$. Fig. 4 shows an 8-PSK constellation using Gray mapping. The signal vectors and orthonormal functions are given by

$$X_m = (x_{m1}, x_{m2}) \tag{12}$$

where, $x_{m1} = \sqrt{E_s}\cos(2pm/M)$ with $\Theta_1(t) = \sqrt{2/T}\cos(w_0 t); 0 \le t \le T$, (13)

$x_{m2} = \sqrt{E_s}\sin(2pm/M)$ with $\Theta_1(t) = \sqrt{2/T}\sin(w_0 t); 0 \le t \le T$.

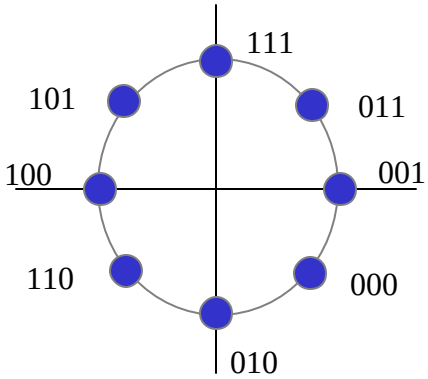

Fig. 4. 8-PSK constellation with gray mapping

The probability of bit error $P_b(k)$ for MPSK signaling over a Gaussian channel using gray mapping can be approximately analytically [23] and for given value of E_s / N_0 is

$$P_b(k) \approx 2Q\left(\sqrt{2E_s / N_0}\sin(\frac{p}{M})\right) \quad (14)$$

Applying the JSCC Scheme, we optimize the minimum rate distortion for different MPSK modulations;

$$D_{unc,\min}(E_s / N_0) = \underbrace{\min}_{k}\{D(1,k)\} \quad (15)$$

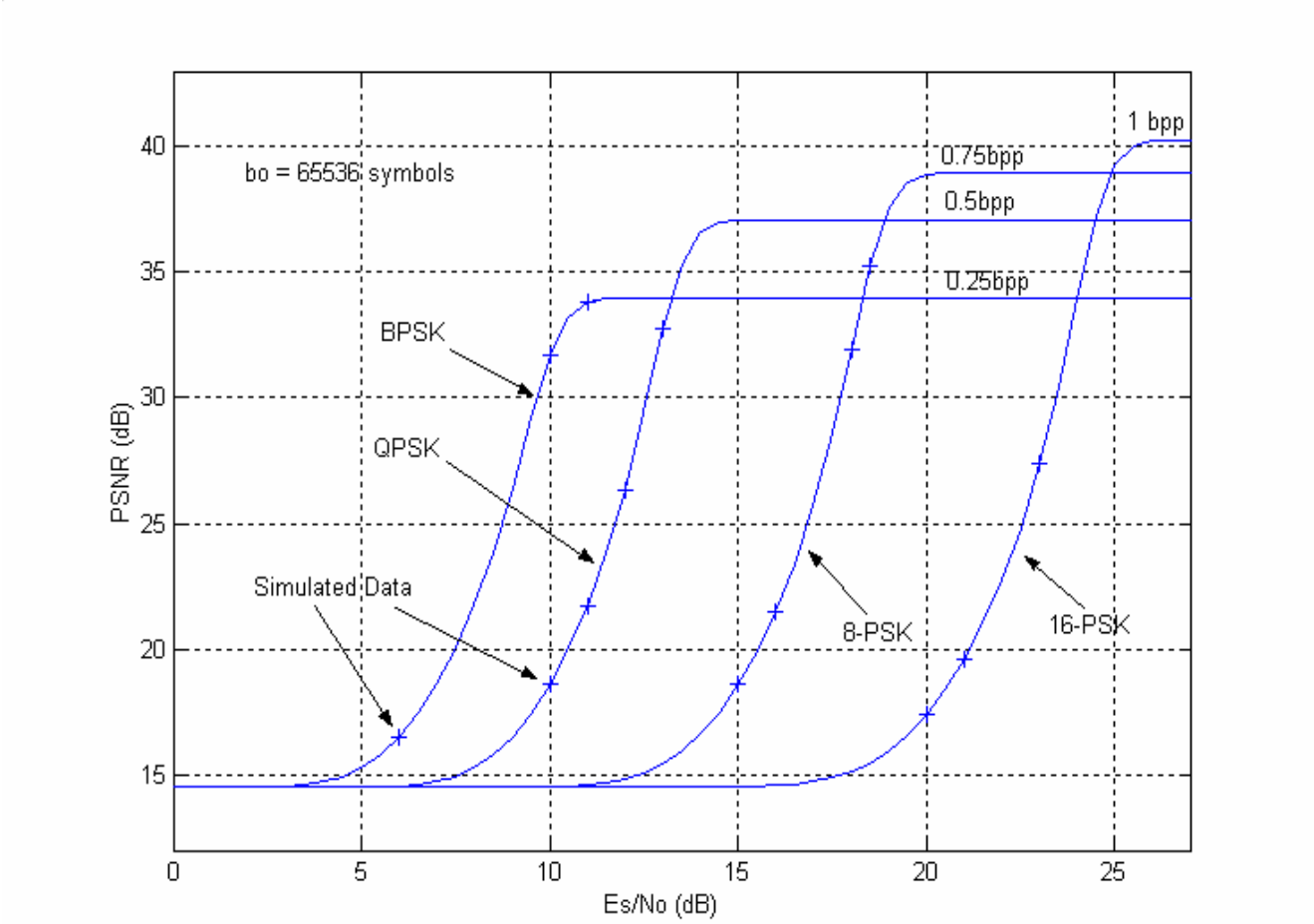

Fig. 5. Performance of uncoded MPSK

Fig. 5 shows the performance of the JSCC scheme by transmitting the Lena image with MPSK modulation over the channel. Also shown are the simulated results and the corresponding theoretical values. However, the performance of this system in terms of Es/No and PSNR is very low: for a PSNR of 33.9 dB we require power of 11.6 dB. To over come this performance issue, coded modulation techniques like TCM are used as explained in the next section.

3.2 Trellis Coded Modulation

The performance of a transmission system can be improved effectively by adding controlled redundancy. Redundancy makes some symbols patterns invalid, thus allowing the receiver to detect, and in some cases correct, the errors introduced by noisy channel. However this addition of redundant bits results in bandwidth expansion that is not desirable, as in our case also, for bandwidth-limited systems. One alternative is to reduce the information rate to make room for the redundant bits, but in many applications this is either extremely difficult or impossible. TCM provides a powerful, additional alternative. G. Ungerboeck [14] introduced the redundancy required for error control without increasing the signal bandwidth by concatenating a convolutional coder with an extended signal mapper. If the uncoded system uses a 2^k-ary signal constellation, TCM encoder added a bit redundancy to every k source bits, expands the signal constellation from 2^k to 2^{k+1} and maps the k+1 encoded bit to the expanded constellation.

The symbol mapping is done in a special way called Set Partitioning. It increases the intra subset Euclidean distance. In Fig. 6, the signal partition tree for 16-PSK constellation is shown. Each partition results in an increase of minimum distance between constellation points. Also, since a convolutional encoder can be presented as a state diagram [24]: An output from convolutional encoder represents a state transition. Therefore, every state will branch out to different states depending upon the input. This fact along with set partitioning principle is carefully used to assign symbols within same subset, which have maximum distances, to the outputs when two branches emerge or converge at a state. This selection ensures a maximum distance called *minimum Euclidean distance* between any two paths in the state trellis that emerge from a state and then re-emerge back later. As the performance of convolutional code is dominated by Euclidean distance [24], this careful selection of symbols and design of encoder results in improved performance. The encoder is designed by an exhaustive computer search in order to maximize the minimum Euclidean distance.

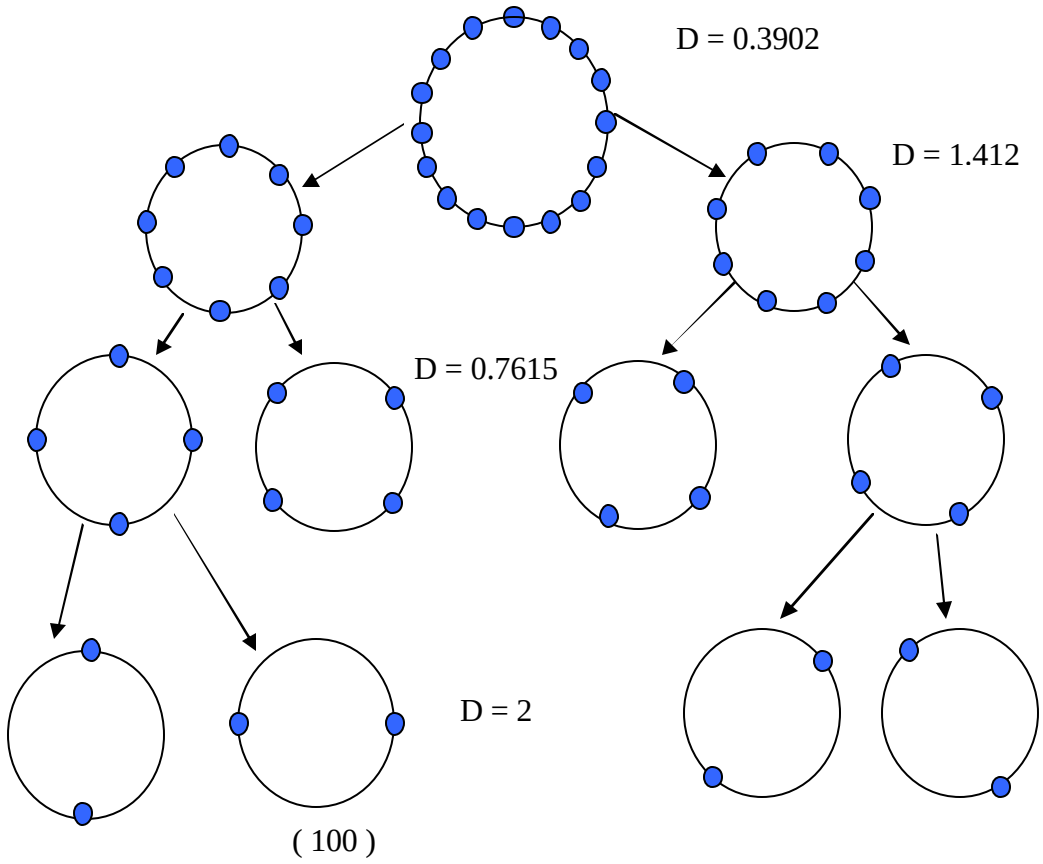

Fig. 6. A partitioning of 16-PSK constellation

G. Ungerboeck [14] also showed that with generic encoder modulator of Fig. 7 for an integer number of bits per second or Hertz, it was possible to achieve Asymptotic Coding Gain (ACG) of as much as 5.8 dB in Es/No with in precisely the same signal spectral bandwidth. The Trellis encoder maps x_1, x_2… x_m input bits onto a signal from 2^{m+1}-ary constellation. A k/(k+1) convolutional coder is used to encode *k* out of *m* information bits. The resulting (k+1) output bits are used to select one of the 2^{k+1}

partitions of the 2^{m+1}-ary constellation at the (k+1) level. The remaining (m-k) information bits are then used to select a signal *z* within in the designated partition.

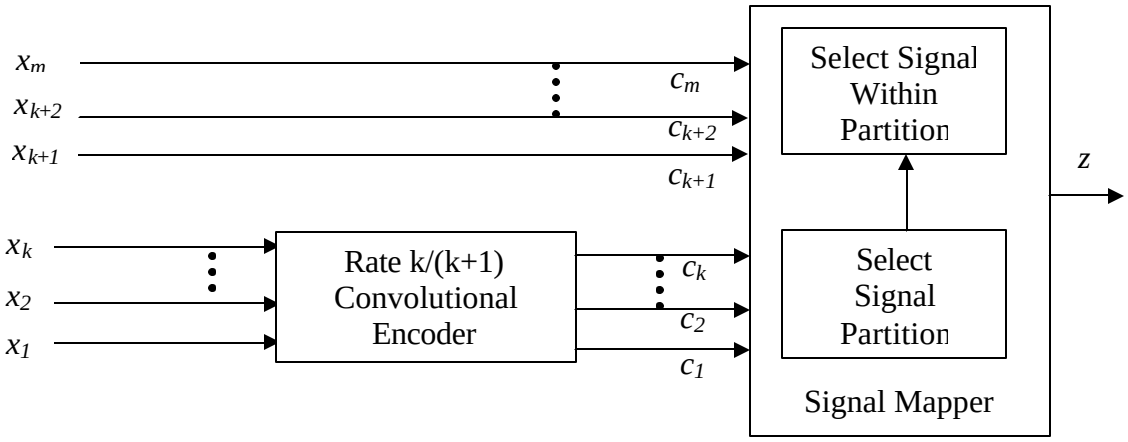

Fig. 7. An Ungerboeck encoder

The decoding of trellis-coded signals is very similar to that of convolutional codes: The trellis structure imparted on the transmitted sequence by the convolutional encoder allows the use of the soft decision Maximum Likelihood (ML) decoding using Viterbi decoder.

The probability of symbol error for transmission over a noisy channel is a function of *minimum Euclidean distance* between the pair of distinct signal sequences. However, because of the (m-k) uncoded bits associated with each trellis states, there can be more than one signal associated with each branch in the trellis; we have signal sequences that differ by a single *parallel partition*. Hence,

$$d^2_{free} = min\,(\, d^2_{free,\,parallel}\,,\, d^2_{free,\,non\text{-}parallel}) \qquad (16)$$

As soft ML-decoding is applied, the node error that a wrong sequence is selected is given over a Gaussian channel by [24]

$$P_b(k) \approx N(d_{free}) Q\left(\sqrt{\frac{d_{free}^2 E_s}{2N_0}}\right) \tag{17}$$

where, $N\ (d_{free})$ is the average number of sequences that are distance d_{free} from the transmitted sequence.

If b_{dfree} is the total number of information bit errors associated with the erroneous path, averaged over all possible transmitted path, we have probability of bit error [24] as

$$P_b(k) \approx \frac{b_{dfree}}{r_c} Q\left(\sqrt{\frac{d_{free}^2 E_s}{2N_0}}\right) \tag{18}$$

Optimizing the rate-distortion function, we have a selection criterion for the JSCC framework given by the following equation

$$D_{cod,\min}(E_s / N_0) = \underbrace{\min}_{r_c,k}\{D(r_c,k)\} \tag{19}$$

Fig. 8 illustrates the gain achieved using TCM codes with MPSK modulation. It also shows the theoretical curve and respective simulations results. There is a mismatch between the theoretical and simulation values at low SNR. It's because the BER equations are approximated using only the error paths at d_{free} distance, however at low SNR, error can occur because of other paths.

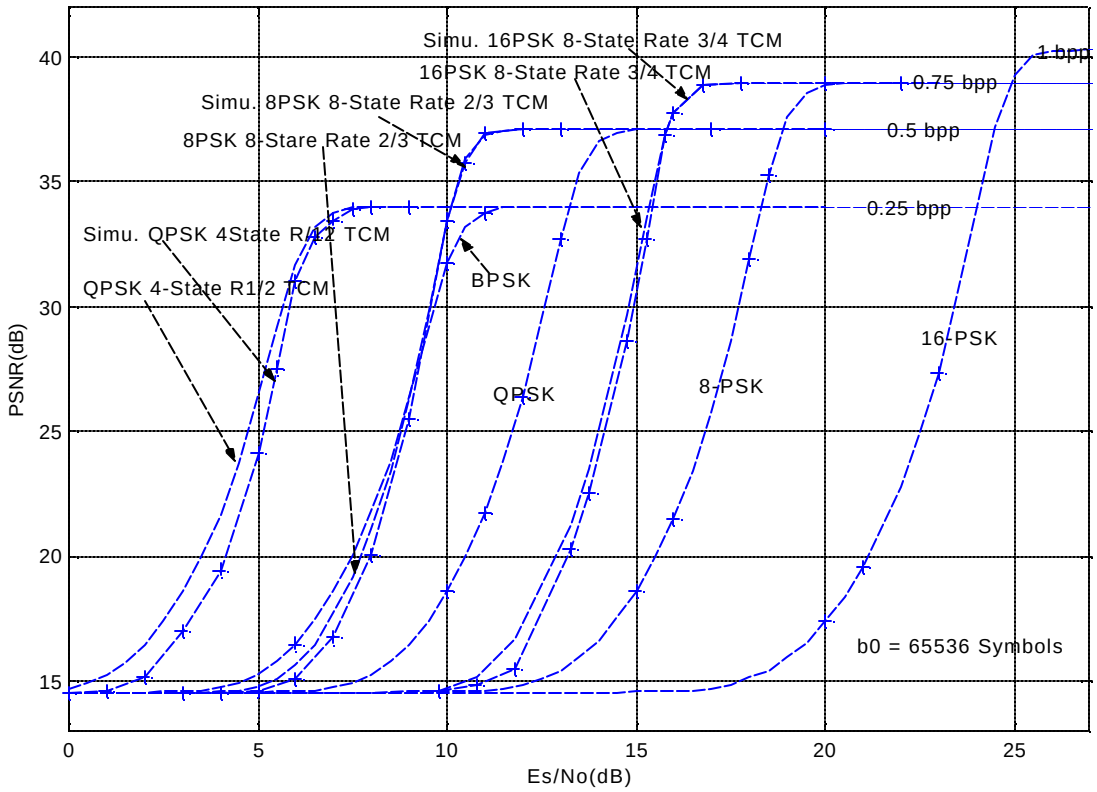

Fig. 8. Performance of TCM

TABLE I

TCM CODES

Uncoded Constellation	Coded Constellation	Coding Gain (dB)	No. Of States
BPSK	QPSK	4	4
QPSK	8-PSK	3.2	8
8-PSK	16-PSK	3.1	8

The Asymptotic coding gain g of TCM can presented as

$$g = \left(\frac{d^2_{free/cod}}{d^2_{free/uncoded}} \right) \tag{20}$$

Table I shows the result of the TCM codes. The performance of TCM codes can be improved by increasing the number of states, effectively increasing the d^2_{free} distance, at the cost of computational complexity. Fig. 9 shows the result of increasing the state size on the performance of rate 2/3 code with 8-PSK signaling. Also, the gains are tabulated in Table II.

TABLE II

EFFECT OF STATE SIZE ON CODING GAIN

Rate 2/3 with 8-PSK mapping						
State size	8	16	32	64	128	256
Coding Gain (dB)	3.2	3.6	3.85	4.01	4.32	4.35

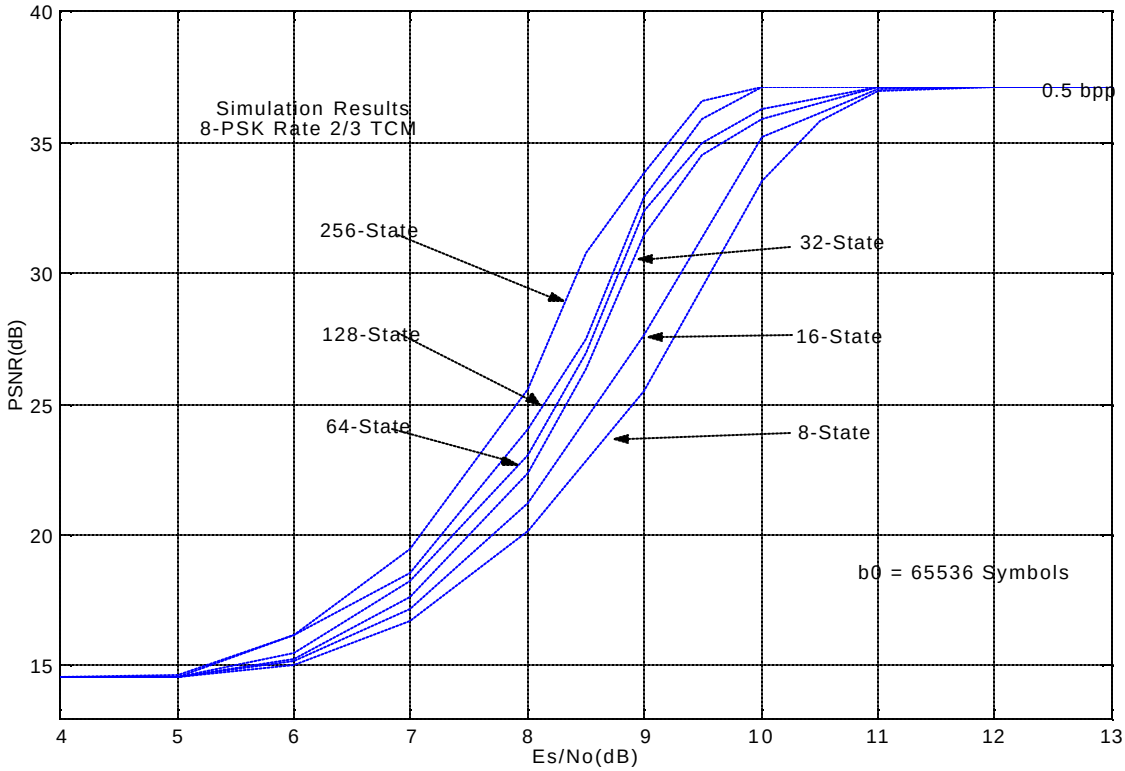

Fig. 9. Effect of d^2free on the performance of TCM

In Fig. 10, the simulation result of using 64-state TCM for different rates (1/2, 2/3 and 3/4 is given) is presented. A 64-state code will be used to design a TCM system employing single encoder-decoder for variable modulation formats as it has reasonable decoding complexity. Table III presents the gain of the 64-state TCM codes.

TABLE III

64-STATE TCM CODING GAIN

Uncoded Constellation	Coded Constellation	Coding Gain (dB)	No. Of States
BPSK	QPSK	5.2	64
QPSK	8-PSK	3.6	64
8-PSK	16-PSK	4.3	64

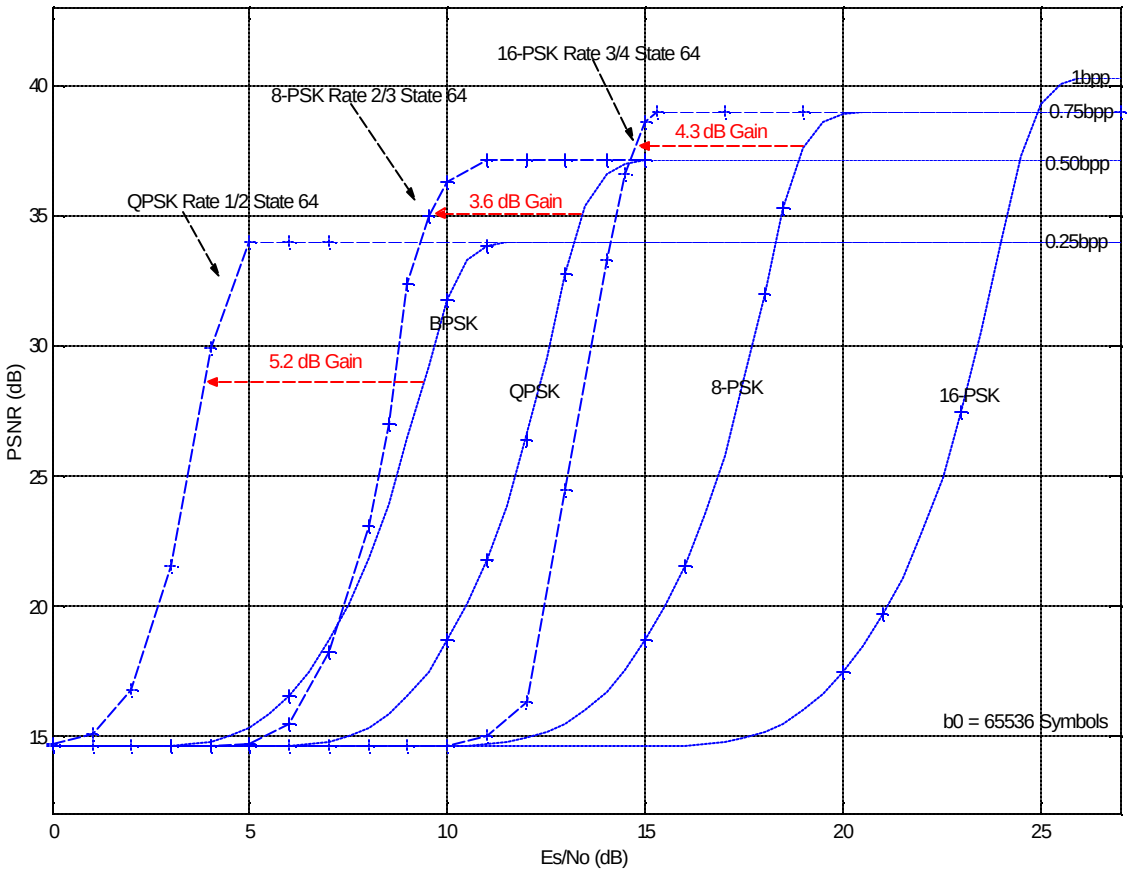

Fig. 10. Ungerboeck's 64-state TCM gain for MPSK modulation

3.3 Punctured TCM Codes

The performance of the TCM system saturates quickly within a narrow range of SNR values. In some cases, as in Fig. 8, the uncoded system may be a better option than coded system. This is highly undesirable, if we want to develop a practical generic TCM system. Another technique is to use punctured codes.

Punctured convolutional codes [25] are often used in practice to reduce the decoding complexity of high-rate codes and to allow a class of variable-rates codes sharing a single encoder-decoder. High rate codes are achieved from puncturing low rate codes by periodically deleting bits from one or more of the encoder output streams. As an example consider the Fig.11: a rate 1/2 code is punctured to produce a rate 2/3 code by deleting periodically the 4^{th} bit of the output stream.

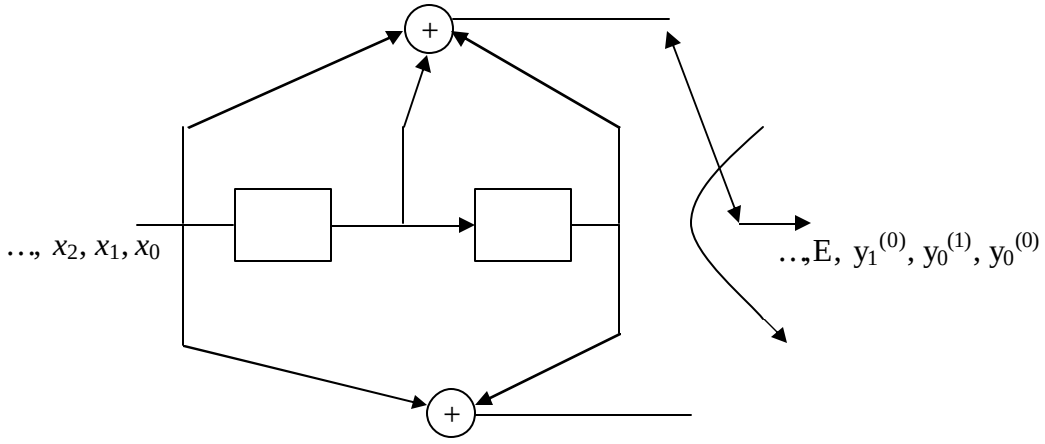

Fig. 11. Puncturing rate 1/2 convolutional code

However, when a code is designed for a specific modulation type, such as in most TCM schemes, using the punctured version of the code may not yield satisfactory results. It is a major drawback of TCM codes that each configuration requires a different code, so that unlike the class of punctured binary codes, no single encoder-decoder could

be used for a wide set of parameter (i.e. 2, 2.5…4 b/s/Hz all with a single decoder). Fig. 12 shows the results of using punctured TCM codes designed to achieve code rate of 2/3 and 3/4 for QPSK, 8PSK and 16 PSK modulations. TCM codes of different state size are used for simulation. They are used because the coded system should be always optimal than uncoded system for all range of SNR values.

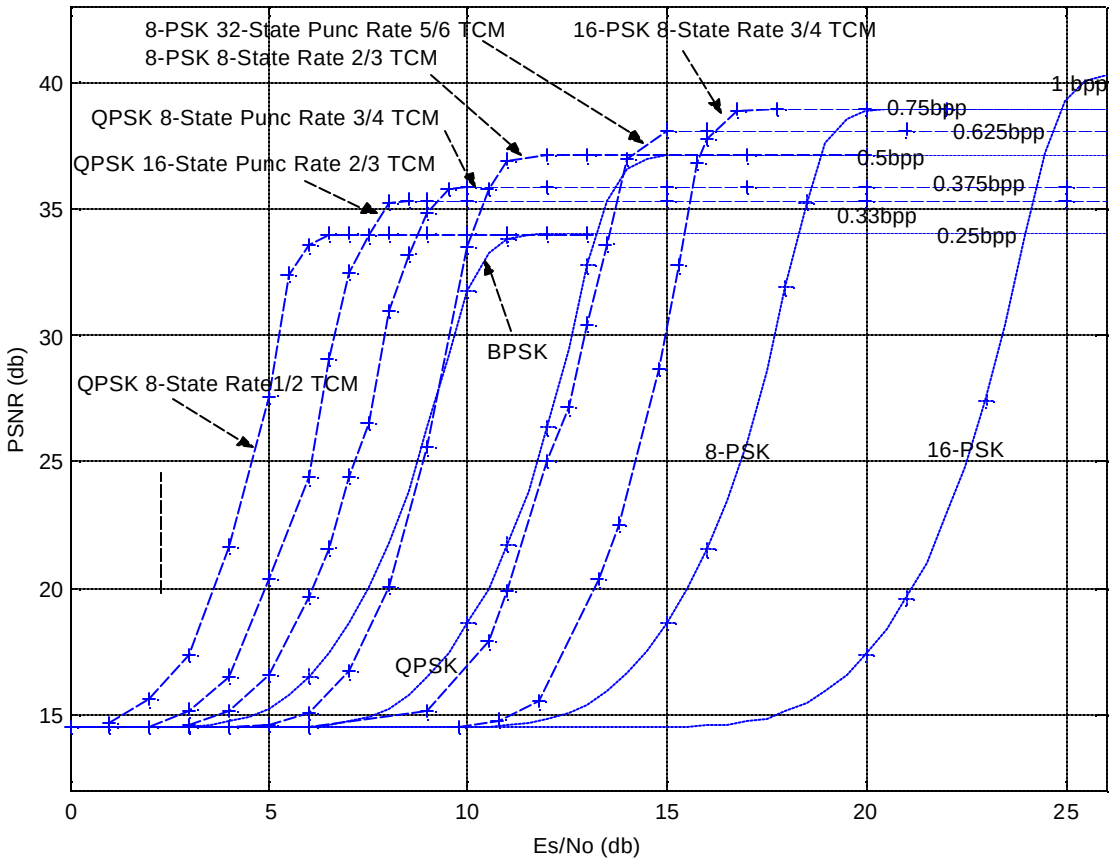

Fig. 12. Punctured TCM

Simulation result of a 64-state TCM code is shown in Fig. 13. A rate 1/2 code is used to generate variable rate TCM codes by puncturing and the resulting punctured TCM codes are then used with various modulation schemes. In the range of 15 to 15.7

dB, uncoded QPSK performs better than TCM system. It is because puncturing rate 1/2 does not produce optimal rate 5/6 code for 8-PSK. Puncturing can also be considered as a part of TCM code design [26], but it does not generate an optimal code for various rates and modulations.

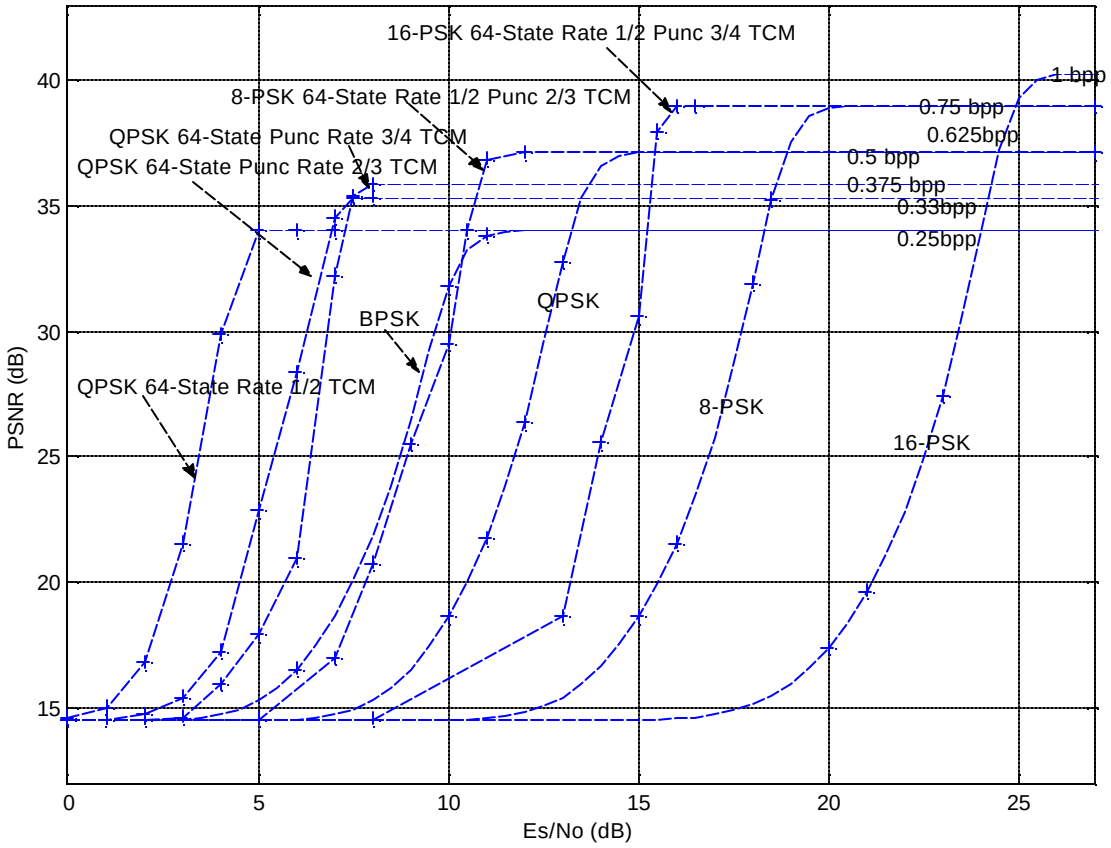

Fig. 13. Punctured 64-sate TCM

High rate codes like punctured rate 5/6 TCM with 8PSK do not perform better because the puncturing decreases d^2_{free} significantly. In order to overcome this shortcoming, Pragmatic and P^2 Trellis codes are used at the cost of some degradation in performance.

3.4 Pragmatic Codes

TCM systems allow for reliable communication at high spectral efficiencies but as the channel improves, it may prove necessary to vary the number of bits/sec/Hz (spectral efficiency) being transmitted to maintain reliability. A TCM system with adjustable spectral efficiency must be designed that can readily adapts to the channel conditions. Punctured TCM codes can be used but they do not usually provide good performance for wide range of spectral efficiency as we have seen in the previous section. A. J. Viterbi et, al. [17] designed a Pragmatic Trellis Code that can adapted to different MPSK constellation by using a rate 1/2 constraint-length-7 Trellis Code, at the loss of some performance. Pragmatic Code design can be explained through Fig. 14. With k-1 input bits, only the lowest order bit is going through binary convolutional encoder, while the remaining k-2 bits select 2^{k-2} signal partition sectors.

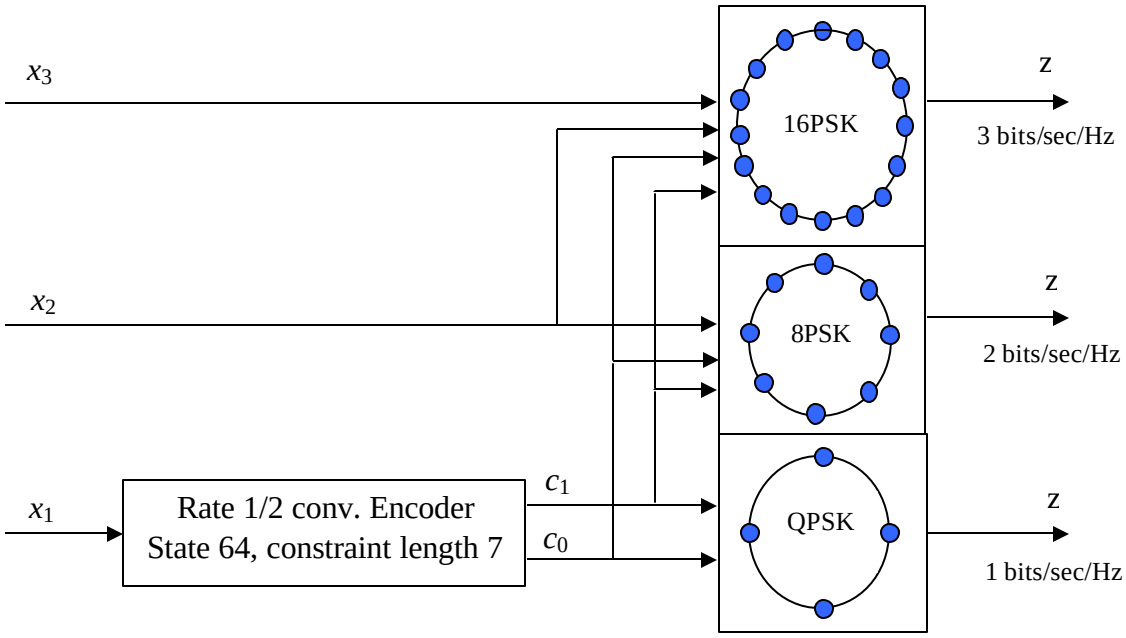

Fig. 14. Pragmatic TCM code structure

The trellis generated by this encoder/modulator will cause parallel transitions: uncoded bits are used to select signal partition sector (higher modulation schemes). Hence, the pragmatic code has a designed constraint: d^2_{free} in worst case must be at least that of parallel transitions.

The trellis code for M = 8 constellation has twice as many branches between states with same connectivity as compared to the trellis of M = 4 constellation. Also, for M = 16 constellation, the trellis code has four parallel branches representing the 2 uncoded input bits. Thus, the d^2_{free} between these four parallel branches is proportional to $\sin^2(\pi/4)$. Similarly, for $M = 2^k$

$$d^2 free \quad \propto \quad \sin^2(4\pi/M) \tag{21}$$

Considering only the minimum Euclidean distance between the parallel transitions, the P_b for TCM can be lower bounded [17] as

$$P_{cu} > KQ\left(\sqrt{(2E_s/N_0)\sin^2(4\pi/M)}\right) \tag{22}$$

where as the BER P_{bu} for an uncoded *M-ary* PSK is bounded [23] by:

$$Q\left(\sqrt{(2E_s/N_0)\sin^2(2\pi/M)}\right) < P_{bu} < 2Q\left(\sqrt{(2E_s/N_0)\sin^2(2\pi/M)}\right) \tag{23}$$

The Asymptotic Coding Gain (ACG) is given as

$$\mathrm{ACG} \le 10\log_{10}\left[\frac{\sin^2(4\pi/M)}{\sin^2(2\pi/M)}\right] \tag{24}$$

$$\cong 10\log_{10}\left[4\cos^2(2\pi/M)\right] \quad M \ge 8 \tag{25}$$

Table IV compares the performance of Pragmatic TCM codes and Ungerboeck's TCM codes. The TCM system designed using pragmatic code can result in a sub-optimal 8-PSK system. However, the efficiency of the adaptive system is more than the loss.

TABLE IV

BER GAIN OF PRAGMATIC CODES

ACG	Ungerboeck Code	Pragmatic Code
8-PSK constellation	5	3
16-PSK constellation	5.6	5.3

Fig. 15 shows the performance of rate 3/4 code 8-state with 16-PSK mapping generated using pragmatic approach from a rate 2/3 TCM. It also shows the theoretical and simulated result. The rate 3/4 code has a coding gain of 3.3 dB where as Ungerboeck's 8-State-16-PSK code has a coding gain of 4.01 dB. A loss of 0.7 dB is incurred, however a single TCM system is now used for both mappings: 8-PSK and 16-PSK. This example demonstrates the effectiveness of the underlying concept. Similar concept is used to generate higher rate TCM codes (5/6,8/9,7/8,11/12 etc) as illustrated in next section.

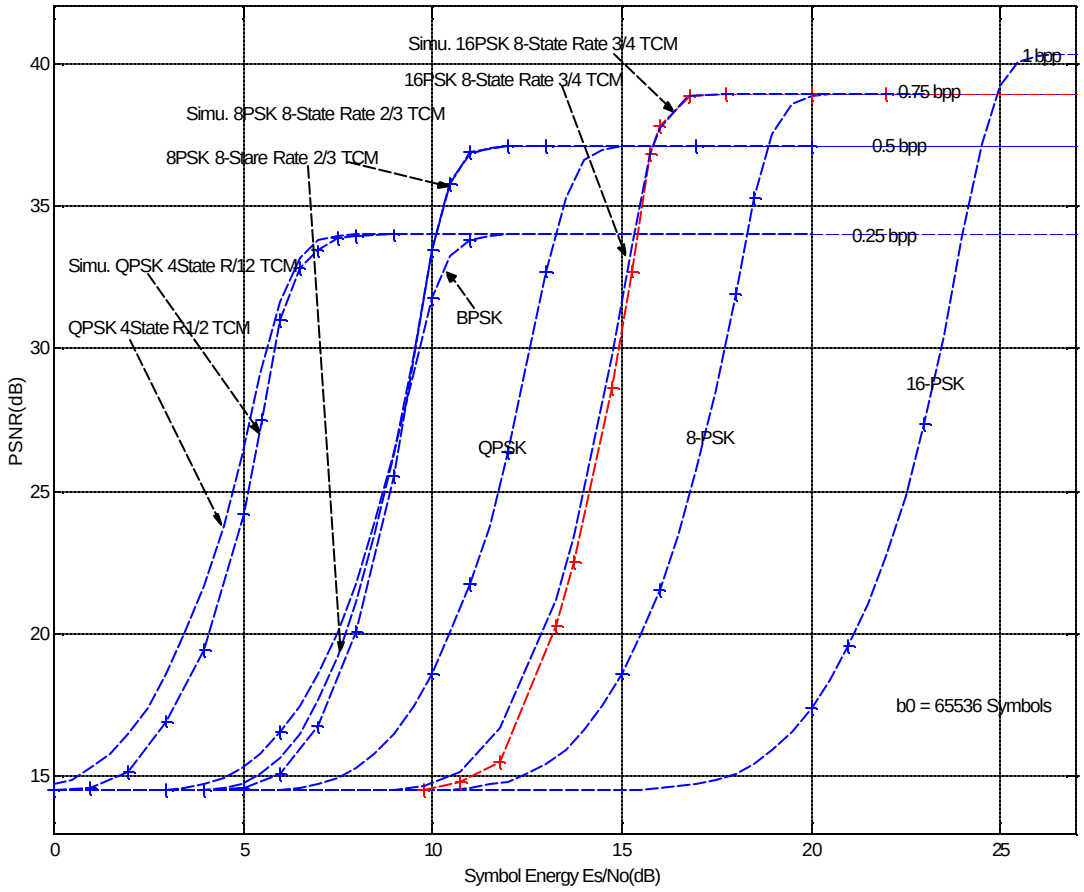

Fig. 15. Pragmatic TCM code (16-PSK 8 state Rate 3/4)

3.5 P [2] TCM Codes

Pragmatic Trellis code could be extended to a wide range of high-rate punctured trellis codes [18] for both PSK and QAM modulation. Puncturing Trellis Code to generate higher rates codes directly reduces the Euclidean distance significantly, therefore, decreasing the performance. However, puncturing a rate 1/2 codes to rates like 2/3 & 3/4 and using the pragmatic approach can lead to good high rate trellis codes. We can therefore, design a TCM system with a single encoder-decoder, which provides variable spectral efficiency depending upon the channel condition.

The performance of trellis system will depends on the minimum Squared Euclidean distance of parallel transition and non-parallel transition in the trellis.

$$d^2(k) = \dim(d_p 4\sin^2(2p/2^{k+1}), 4\sin^2(2p/2^{p+1})) \tag{26}$$

Consider an example of Rate 5/6 P^2 TCM code designed for 8-PSK shown in Fig. 16. A rate half code is punctured to produce rate 3/4 code. These 4 outputs along with 2 uncoded bits are mapped into two 8-PSK symbols. Since, the uncoded 8-PSK can transmit information at 3 bit/Hz; this scheme will transmit at rate of 2.5 bit/Hz. Assuming that the 8-PSK constellation are uniformly distributed on the circle,

$$d^2_{parallel} = 4 \tag{27}$$

The Hamming distance of rate 1/2 64-state code (de facto industry standard code) punctured to rate 3/4 is 5. Thus,

$$d^2_{free,parallel} = 5\times(2\sin(2p/8))^2 = 2.929 \tag{28}$$

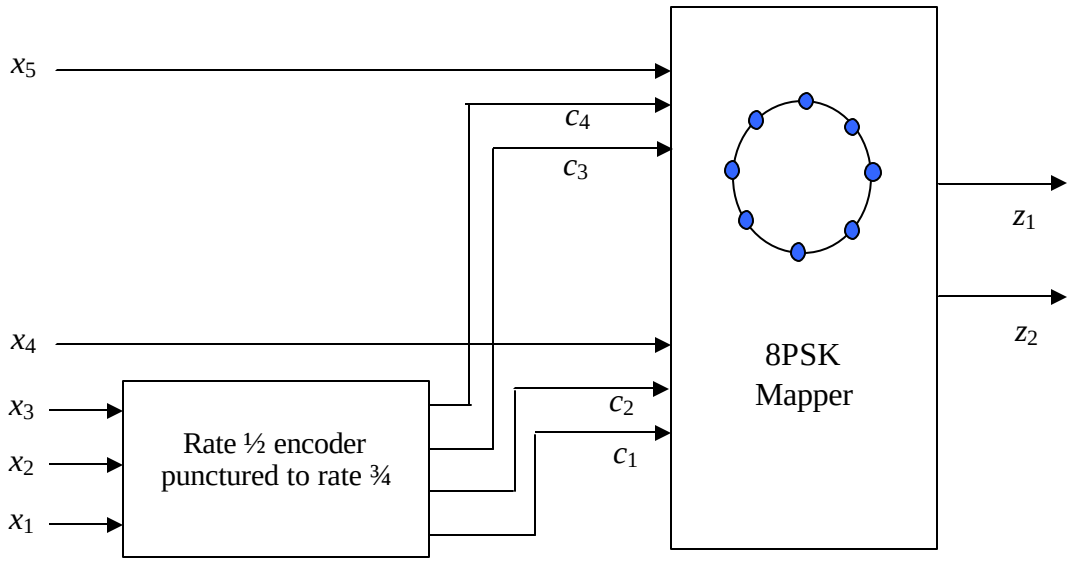

Fig. 16. Rate 5/6 8-PSK P^2 TCM code

Since, the uncoded QPSK modulation has a free squared Euclidean distance of 2, therefore, the 5/6 P^2 code has higher information rate and ACG as compared to uncoded QPSK modulation.

The same concept is used to design rate 5/6 code from rate 1/2 code. The performance of this code compared to uncoded QPSK system is shown in Fig. 17. A gain of 1.3 dB is achieved. Using similar approach, higher rate codes like 5/6,8/9,7/8,11/12 etc can be designed for various modulation formats. A TCM PSK system (single encoder-decoder) is now presented, based on TCM, punctured TCM, Pragmatic TCM and P^2 TCM Codes, which is efficient in terms of power and PSNR as compared to uncoded MPSK system.

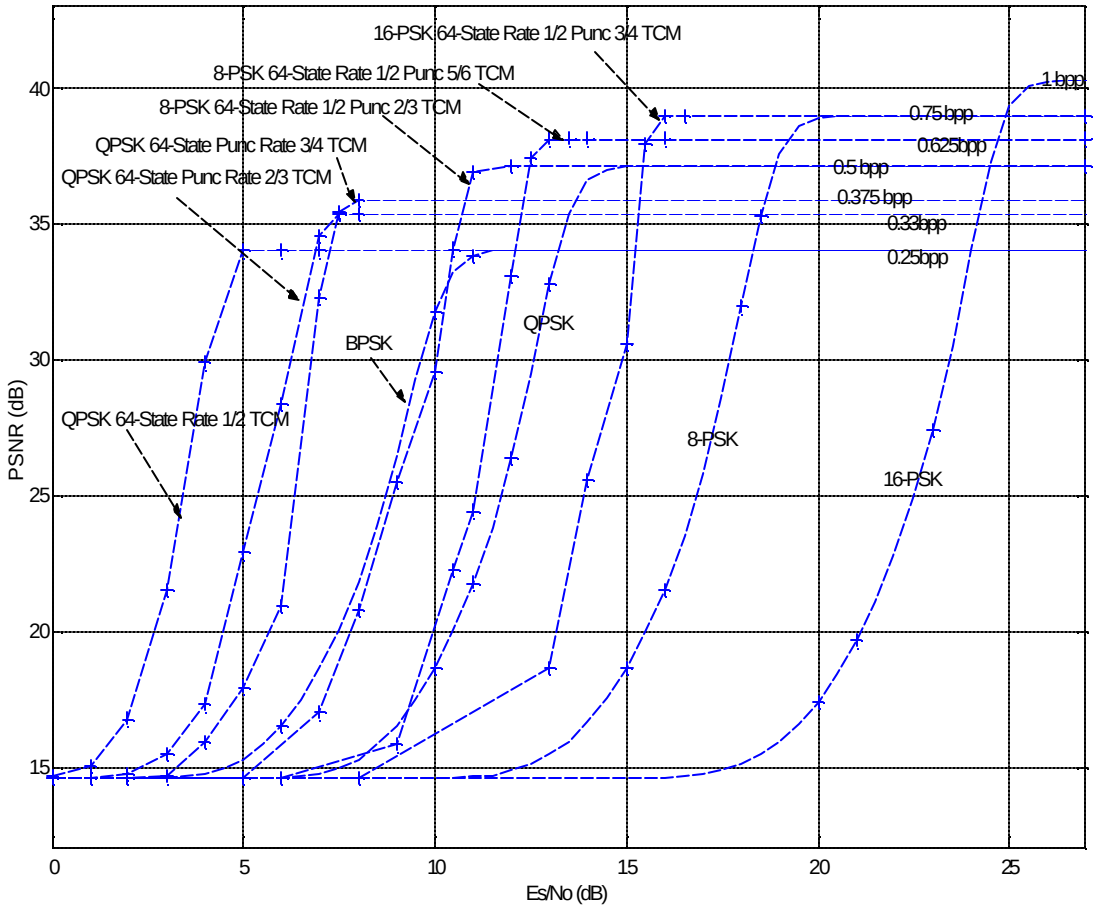

Fig. 17. Performance of P^2 rate 5/6 8-PSK TCM code

3.6 Adaptive TCM System

The design of an adaptive TCM system is presented that outperforms uncoded MPSK signaling for any given value of Es/No and distortion using different rates and constellation sizes. Fig. 17 shows the generic TCM system. Depending upon value of Es/No, optimal performance in terms of minimum distortion can be achieved. The TCM encoder used is de facto industrial standard rate 1/2 state-64 TCM [17].

The operation of adaptive TCM system is summarized in Table V.

TABLE V

TCM SYSTEM

Es/No Range (dB)	Code Rate (r_c)	Source Rate (r_s)	Signal Constellation
0.00-6.91	0.50	0.250	QPSK
6.91-7.48	0.66	0.330	QPSK
7.48-10.8	0.75	0.375	QPSK
10.8-12.45	0.66	0.500	8-PSK
12.45-15.6	0.75	0.625	8-PSK
15.60-25.00	0.75	0.750	16-PSK

So far, the performance of the JSSC scheme employing TCM system is studied in terms of BER (Es/No). In the following chapter, the performance is analyzed from channel capacity point of view and powerful codes will be used to come closer to the capacity.

CHAPTER IV

CAPACITY ACHIEVING CODES

4.1 Channel Capacity

This Section presents the capacity of a Discrete input Continuous output Memoryless Channel (DCMC) e.g. AWGN. Consider a message block d_m, which is mapped into a transmitted waveform $x_m(t)$. The received waveform $r_m(t)$, is the transmitted waveform disturbed by AWGN $n(t)$. The received signal is coherently detected and processed to provide an estimate of the transmitted message $\hat{d}_m$.

We assume the set of *M-ary* symbols, $\{X_m(t)$; m =1… M$\}$, are finite–energy band-limited waveforms with symbol period T. Application of the Gram–Schmidt orthogonalisation procedure yields a set of orthonormal functions $\{\Theta_n(t)$; n = 1,…..,N$\}$. Each waveform can be expressed as

$$x_m(t) = \sum_{n=1}^{N} x_{mn}\Theta_n(t) \tag{29}$$

with x_{mn} as

$$x_{mn} = \int_0^T x_m(t)\Theta_n(t)\partial t \tag{30}$$

The vector representation of $x_m(t)$ contains coefficients, X_m; $X_m = \{x_{m1}….x_{mN}\}$; m = 1… M. Let the noise process be written as

$$n(t) = \sum_{1}^{N} n_n\Theta_n(t) + \hat{n}(t) \tag{31}$$

The coefficients of the noise process, $\{n_n: n = 1..N\}$, are Independent and Identically Distributed (IID) Gaussian random variables with zero mean and variance $N_0/2$. Demodulation of the received signal involves correlation detection. The correlator outputs are sampled at time, T, to provide the output sample, y, which is processed to yield d_m. The correlator detection removes $\hat{n}(t)$.

The statistic of the Gaussian channel is represented by

$$p(Y/X_m) = \prod_{n=1}^{N} p(y_n / x_{mn}) \tag{32}$$

$$= \prod_{n=1}^{N} \frac{1}{\sqrt{\Pi N_0}} \exp\left(\frac{-(y_n - x_{mn})^2}{N_0}\right) \tag{33}$$

Since,

$$C_{DCMC} = \underbrace{\max}_{p(X_1)\ldots\ldots p(X_m)} I(X;Y) \tag{34}$$

Therefore,

$$C_{DCMC} = \underbrace{\max}_{p(X_1)\ldots\ldots\ldots p(X_m)} \sum_{m=1}^{M} \int_{-\infty}^{\infty} \ldots\ldots \int_{-\infty}^{\infty} p(Y/X_m)\, p(X_m) \log_2\left(\frac{p(Y/X_{m)}}{p(Y)}\right) \partial Y \tag{35}$$

Putting the Channel Statistics, we get the required channel capacity equation

$$C_{DCMC} = \log(M) - \frac{1}{M\left(\sqrt{\Pi}\right)^2} \sum_{m=1}^{M} \int_{-\infty}^{\infty} \ldots\ldots \int_{-\infty}^{\infty} \exp(-|T|^2) \log_2\left(\sum_{i=1}^{M} \exp(-2T \cdot D_{mi} \cdot - |D_{mi}|^2\right) \partial T \tag{36}$$

where $D_{mi} = \left(X_m - X_i\right) \Big/ \sqrt{N_o}$ and with new variable of integration $T = (t_1, t_2, \ldots, t_N)$.

4.1.2 Phase Shift Keying

Phase shift keying (PSK) is a scheme where the information is contained in the phase of the transmitted carrier. The set of waveforms is described by

$$x_m(t) = \begin{cases} \sqrt{\frac{2E_s}{T}}\cos(w_o t - 2pm/M);\ 0 \le t \le T; \\ 0 \qquad\qquad\qquad\qquad ;\ \text{Otherwise} \end{cases} \tag{37}$$

In Fig. 18, the channel capacity for MPSK is shown and the corresponding performance of the JSCC framework employing TCM system and uncoded system is shown in Fig. 19.

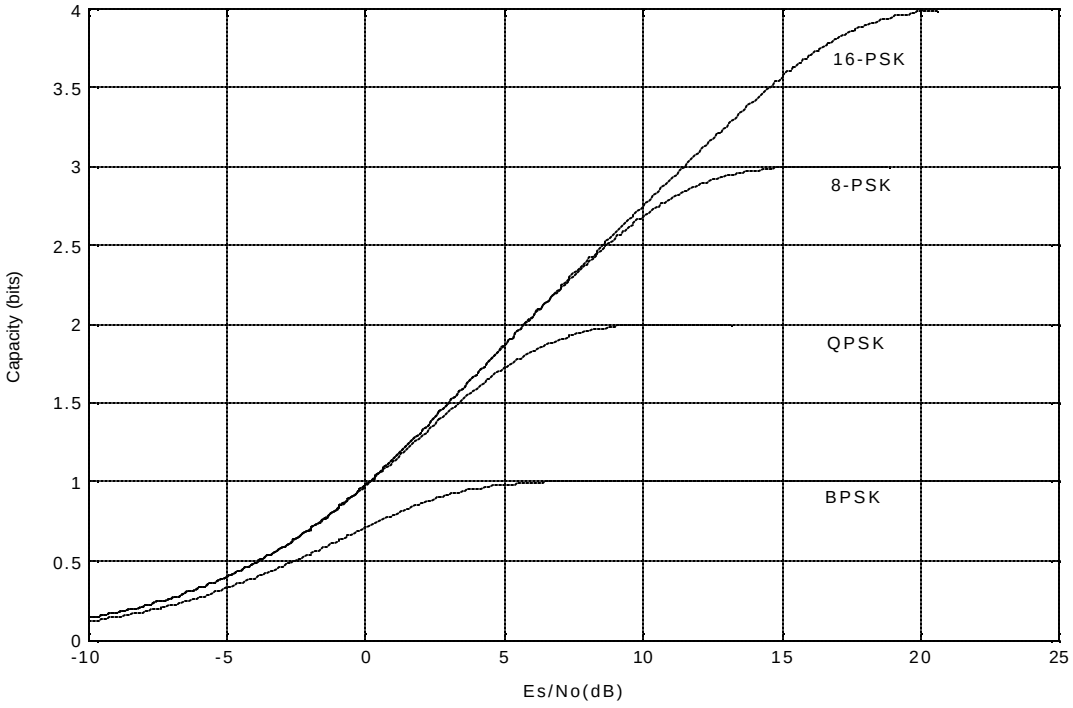

Fig. 18. Channel capacity of MPSK

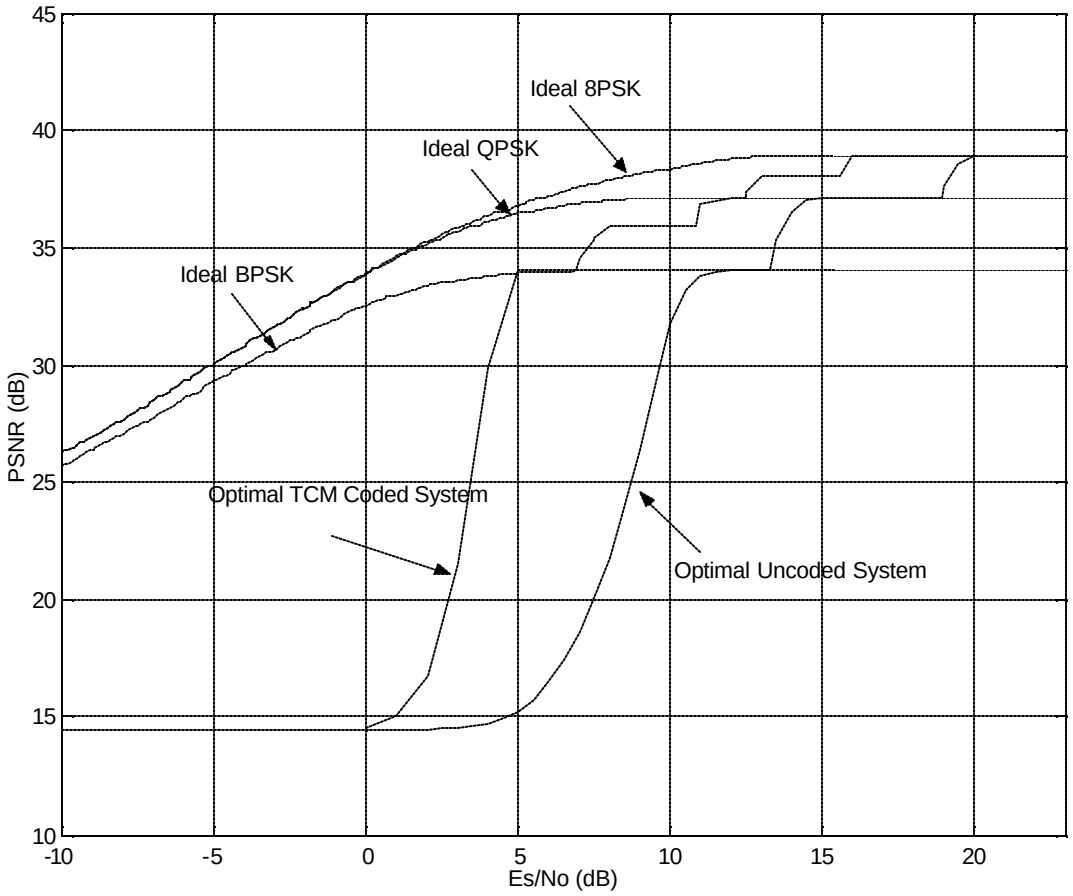

Fig. 19. Capacity achieved by JSCC scheme

These results are also reported in [27]. There are large SNR-Gaps at low values of SNR. Performance can be improved by employing capacity-achieving codes like Turbo and LDPC codes for low values of Es/N_0. TCM codes were used because simulations can verify theoretical bounds (Fig. 8). Better results are obtained by replacing the TCM codes with the LDPC or Turbo codes, but these have looser theoretical bounds, as shown in following sections.

4.2 Turbo Codes

Coding theorist have traditionally attacked the problem of designing good codes by developing codes with lots of structure, which lends itself to feasible decoders, although coding theory suggests that codes chosen at random should perform well if their block size is large enough. The challenge to find practical decoders for almost random, large codes has not been seriously considered until recently. C. Berrou et al. [19] introduced turbo codes in 1993, which achieve near Shannon-limit error correction performance with relatively simple component codes and large interleaver. The introduction of turbo codes has opened a whole new way of looking at the problem of constructing good codes and decoding them iteratively with low complexity.

4.2.1 Turbo Encoder

A turbo encoder consists of two binary rate 1/2 convolutional encoders separated by an N-bit interleaver, together with an optimal puncturing mechanism as shown in Fig. 20. A recursive systematic convolutional (RSC) coder is used. Parity bits (RSC coder output bits) and systematic bits are the outputs of turbo encoder.

RSC structure is needed to produce good rate 1/2 constituent codes. By good constituent codes we mean codes with maximum effective free distance *dfree*, these codes maximize the minimum output weight for weight-2 input sequences: Because this weight tends to dominate the performance characteristics over the region of interest

Although, an RSC can output some bad weight-2 codes but with the introduction of interleaver between 2 RSC codes, the chances of getting a bad weight-2 output sequences from turbo codes is fairly low. This clever use of interleaver boosts the performance of turbo codes. Asymptotically, the BER performance of turbo codes can be approximated [28] as,

$$P_b \approx \frac{N_{free}\tilde{w}_{free}}{N} Q\left(\sqrt{d_{free}\frac{2rE_b}{N_0}}\right) \tag{38}$$

where w_{free} is the average weight of messages whose code word has distance d_{free} and N_{free} is the average number of code words at that distance d_{free}.

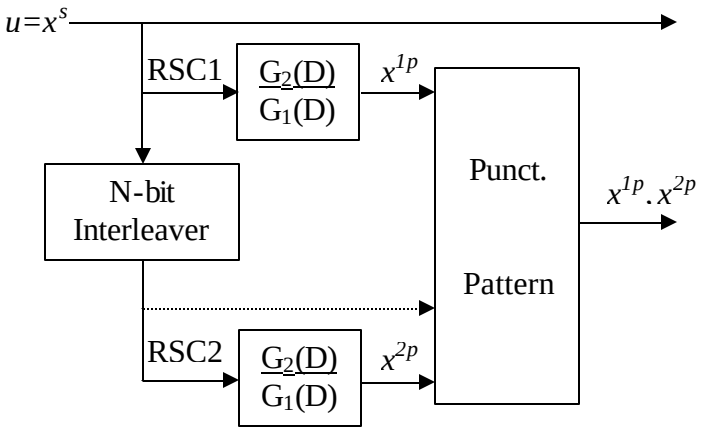

Fig. 20. Turbo encoder

4.2.2 Turbo Decoder

Unfortunately, the presence of an interleaver immensely complicates the structure of a turbo code trellis; a decoder based on ML sequence estimate cannot be used, hence a sub-optimal iterative decoding based on binary BCJR [29] A Posteriori Probability (APP) algorithm is proposed. The APP decoder estimates the bit probability given the channel output sequence. The turbo decoder follows the same structure as of turbo encoder: two APP decoders separated by an interleaver. Each decoder receives

Log-Likelihood Ratio (LLR) of the bits generated by corresponding encoder as shown in Fig. 21. Also, extrinsic information is provided about the parity bit of other decoder. This soft information is used to increase the estimate of the bit LLR values. The turbo decoder iterates until either the solution converges to true estimate of bit LLR or stopping criteria is achieved. A hard decision follows to decide the estimate of the information bits: input to the turbo encoder.

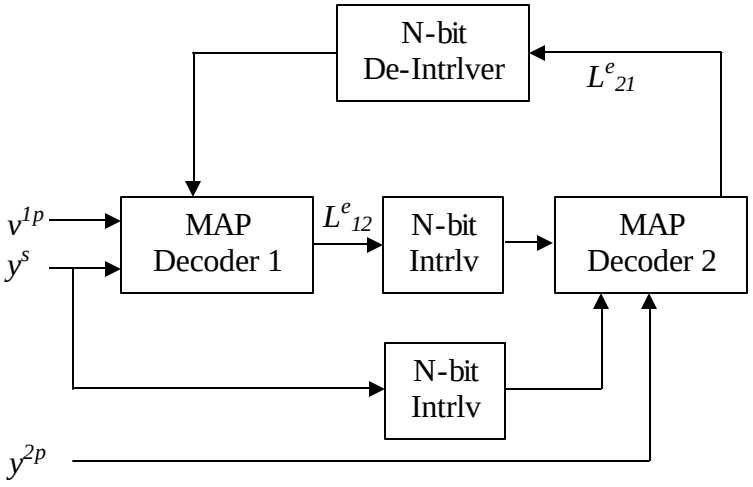

Fig. 21. Turbo decoder

4.2.3 Turbo Coded Modulation

In the case of coded modulation with Turbo codes, there are a couple of techniques that can be followed. A turbo system can be designed specific to the corresponding modulation used [30]-[36]: a symbol interleaver is used and a symbol BCJR algorithm is replaced at the decoder side. A simple technique [37] is direct

extension of binary Turbo codes as shown in Fig. 22. The output of binary turbo encoder is mapped to some constellation symbols. The received symbols are demodulated and a Log-Likelihood Ratio (LLR) of each bit in the symbol is computed. This soft information is now passed to the decoder. Now instead of producing the soft information in the turbo decoder, as in the case of binary turbo codes, it is generated in the channel demodulator. This soft information is used by the binary turbo code to decode the bits. This scheme is simple and easily extendable.

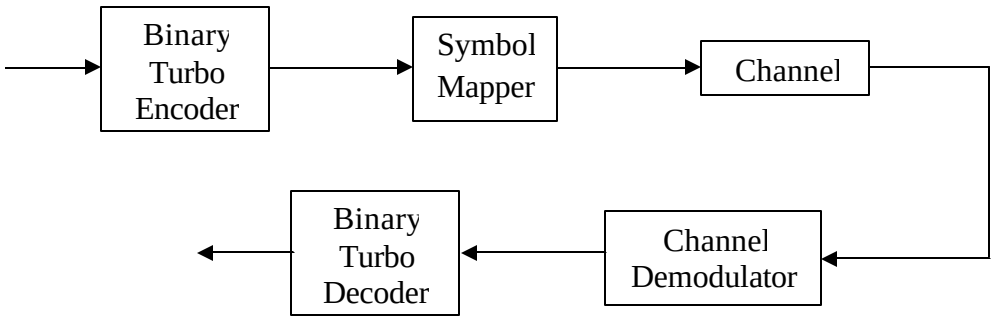

Fig. 22. Coded modulation with Turbo codes

Turbo codes for rate 1/2 16-State QPSK and rate 1/3 & rate 2/3 with 16-State 8PSK are designed using this technique. The performance using an S-random interleaver with a block size of 6K is shown in following Fig. 23 and Fig. 24. Also, the coding gain is given in Table VI. The rate 1/3 code is 1.77 dB away from capacity where as rate 1/2 and rate 2/3 codes are 1.2 and 1.36 dB respectively away from capacity. The performance for such system degrades at low SNR because of increased noise power.

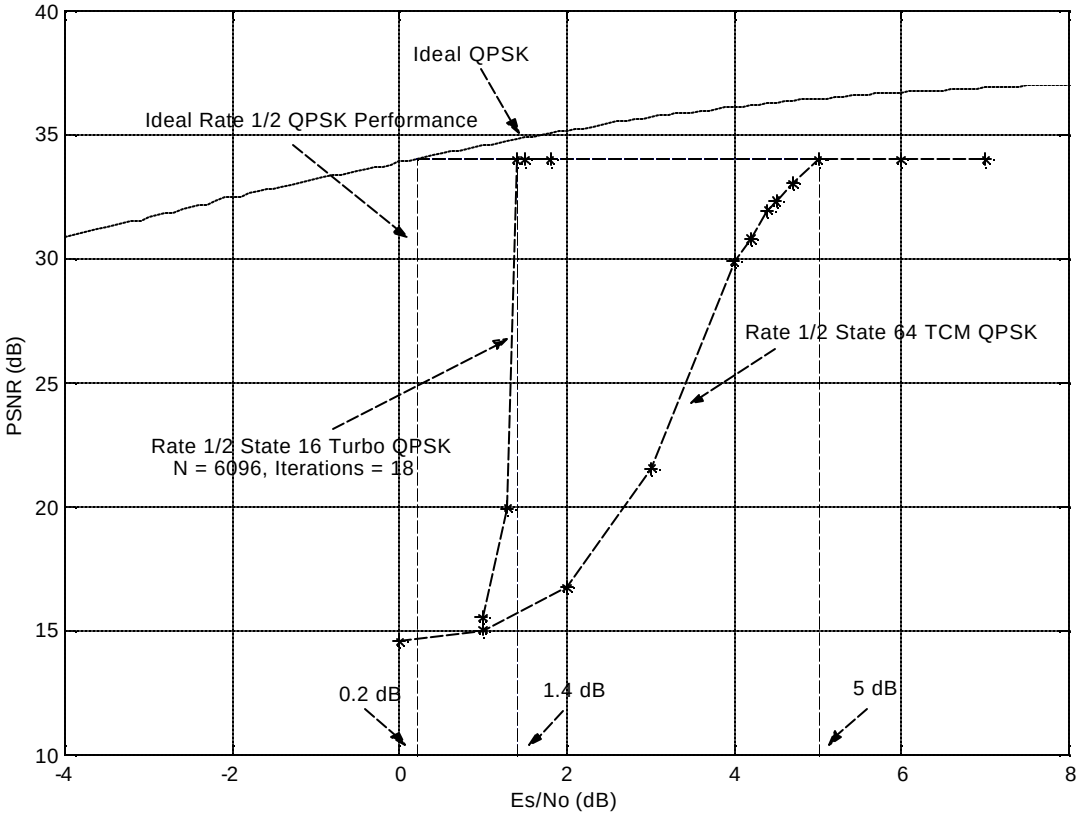

Fig. 23. Performance of rate 1/2 16-state QPSK Turbo code using N = 6000

TABLE VI

TURBO CODING GAIN

Signal Constellation	Code Rate (r_c)	Gain from TCM MPSK System (dB)	Gain from Uncoded MPSK System (dB)	SNR-GAP (dB)
QPSK	0.5	3.6	8.8	1.2
8-PSK	0.66	4.2	7.4	1.36
8-PSK	0.33	-	-	1.77

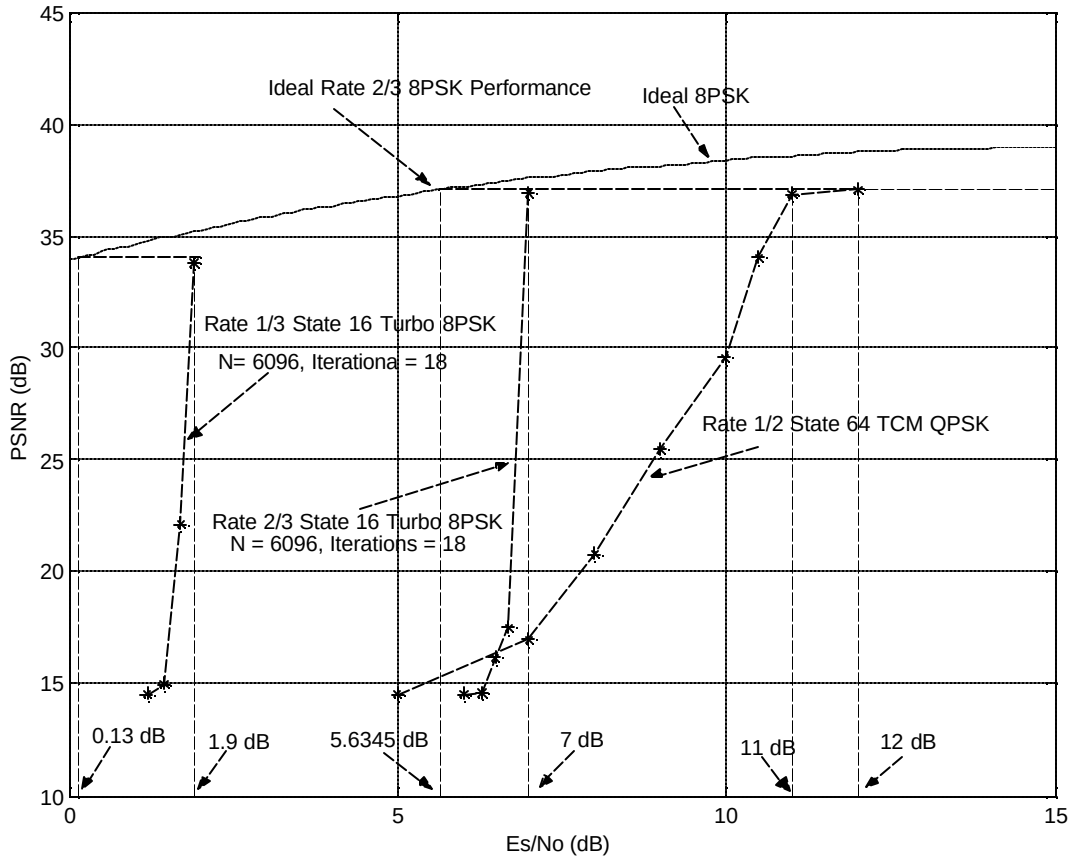

Fig. 24. Performance of rate (1/3,2/3) 16-state 8-PSK Turbo code using N = 6000

Turbo codes with coded modulation can achive a gain of 3 to 4 dB over corresponding TCM Codes as evident from the above Figures. The codes on averge are 1.2 dB away from near-Shannon-limit error correction performance. The gap can be futhur reduced significantly by increasing the frame size but at the cost of exponential increase in computation and latency and/or using turbo codes designed specifically for coded modulation. An alternate is to use low complexity LDPC codes.

4.3 LDPC Codes

Low Density Parity Check (LDPC) codes are linear block codes with a very sparse parity check matrix (H) and were first proposed by R.Gallager in 1963 [22]. Low-density means a low density of 1's in H. In particular, a (*n, k, wc, wr*) low-density code, with *k* input bits and *n* output bits, has *wc* 1's on average in each column and *wr* (>*wc*) 1's on average in each row.

An LDPC codes is completely specified by its parity check matrix. If *wc* and *wr* are fixed for each column and row respectively, we call it a regular LDPC code, otherwise, an irregular LDPC code. Besides the constraint on *wc* and *wr,* the H matrix is constructed randomly. The number of non-zero elements in each row and column of the H matrix specifies an ensemble of LDPC code. If no two columns overlap in more than one row position, the Bit Error Rate (BER) performance of LDPC codes improves [38].

LDPC codes can be effectively presented as a bipartite graph. The bipartite graph is divided in a set of two nodes: variable nodes presenting the column of H matrix and check nodes presenting the rows of H matrix. An edge exists between a variable node and a check node only if the corresponding (row, column) entry in the H matrix is 1. For example, the Fig. 25 shows an H matrix of an LDPC code that is constructed randomly and Fig. 26 shows its equivalent graph representation. If the H matrix has N columns and M rows, the graph will have N variable nodes, M check nodes and the rate of the code will be 1-M/N.

Extensive work [39] has been done on the design of LDPC codes. The performance of regular codes is only slightly inferior to that of turbo codes. However, irregular codes are shown to have much better BER performance compared to regular codes. When designed carefully, the irregular LDPC codes can perform very closely to the capacity for a range of channels.

$$H = \begin{pmatrix} 1 & 1 & 1 & 1 & 0 & 0 & 0 & 0 & 0 & 0 \\ 1 & 0 & 0 & 0 & 1 & 1 & 1 & 0 & 0 & 0 \\ 0 & 1 & 0 & 0 & 1 & 0 & 0 & 1 & 1 & 0 \\ 0 & 0 & 1 & 0 & 0 & 1 & 0 & 1 & 0 & 1 \\ 0 & 0 & 0 & 1 & 0 & 0 & 1 & 0 & 1 & 1 \end{pmatrix}$$

Fig. 25. Parity check matrix

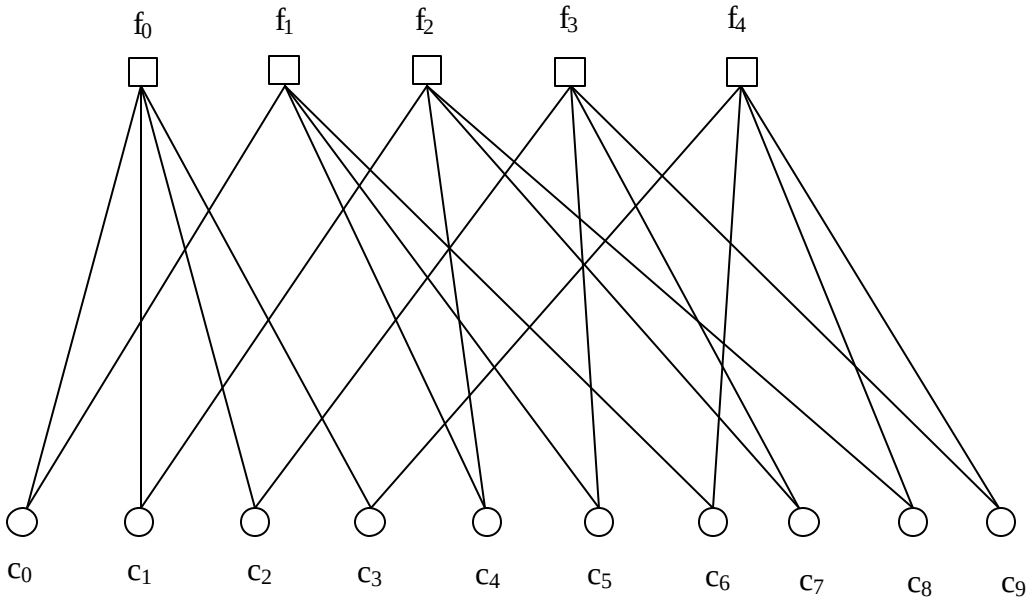

Fig. 26. Tanner graph representation of parity check matrix

4.3.1 Encoding of LDPC

Encoding of the LDPC codes is similar to that of any linear (*N*, *K*) block code. A message vector *m* of length *K* is multiplied with the *K* x *N* generator matrix G of the code to generate the output codeword *c* of length *N*. All the computations are carried over the binary field in the case of binary LDPC codes.

$$C = m\,G \tag{39}$$

The generator G matrix can be readily obtained generated from the parity check matrix (H). The systematic H matrix can be described as,

$$H = [I \mid P] \tag{40}$$

where P is parity check part and I is the (*N* - *K*) x (*N* - *K*) identity matrix.

The generator matrix *G* is then

$$G = [P^T \mid I] \tag{41}$$

where P^T represents the *K* x (*N* - *K*) transposed parity check part and I represent a K x K identity matrix.

Since, the H matrix is constructed as random, therefore in order to get G matrix, it has to be converted to systematic form by applying Gaussian elimination. Even though the systematic form of the H matrix is used for the encoding process, the original random form of the H matrix is used in decoding the codeword because of its sparse nature. When the H matrix is converted to a systematic form, the parity part of the matrix is usually very dense. When the block length is in order of 10^6, LDPC codes have quadratic encoding complexity. However, irregular codes (H matrix) can be designed [40] to have linear encoding complexity.

4.3.2 Decoding of LDPC

The decoding algorithms for LDPC codes work *iteratively*. Information is exchanged between neighboring nodes (variable and check nodes) in the graph by passing messages along the edges.

Initially each message carries the Log Likelihood Ratio (LLR) of the received codeword bits corresponding to the variable node it emerges from. At each check node, the LLR of message, such that the checksum results in a zero, is computed and the extrinsic information is passed onto the message edge. The variable node computes the LLR and passes the extrinsic information along each message edge. The messages carrying the extrinsic information iterates between the nodes. Also, a hard decision based on the messages received at the variable node is made: one can consider the bit's most likely value implied by all messages.

The decoding stops when the checksum, by passing the hard decision along the message edges, at all the check nodes results in all zero output. The BER performance of rate 1/2 LDPC code (regular, irregular) for a block size of 256k bits using codes of [41] is shown in Fig. 27 along with threshold for Turbo Codes. Irregular codes outperform regular codes by 0.62 dB where as regular LDPC codes does not perform better compared to Turbo codes. The results are summarized in Table VII.

TABLE VII

GAIN OF RATE 1/2 LDPC CODE WITH BPSK SIGNALING

LDPC Code	dvmax	Theoretical Limit Threshold (dB)	Simulated (dB)	SNR-GAP (dB)	Gain over Turbo Code (dB)
Irregular	12	0.371	0.507	0.502	0.053
Regular	3	1.1	1.159	0.961	-0.401

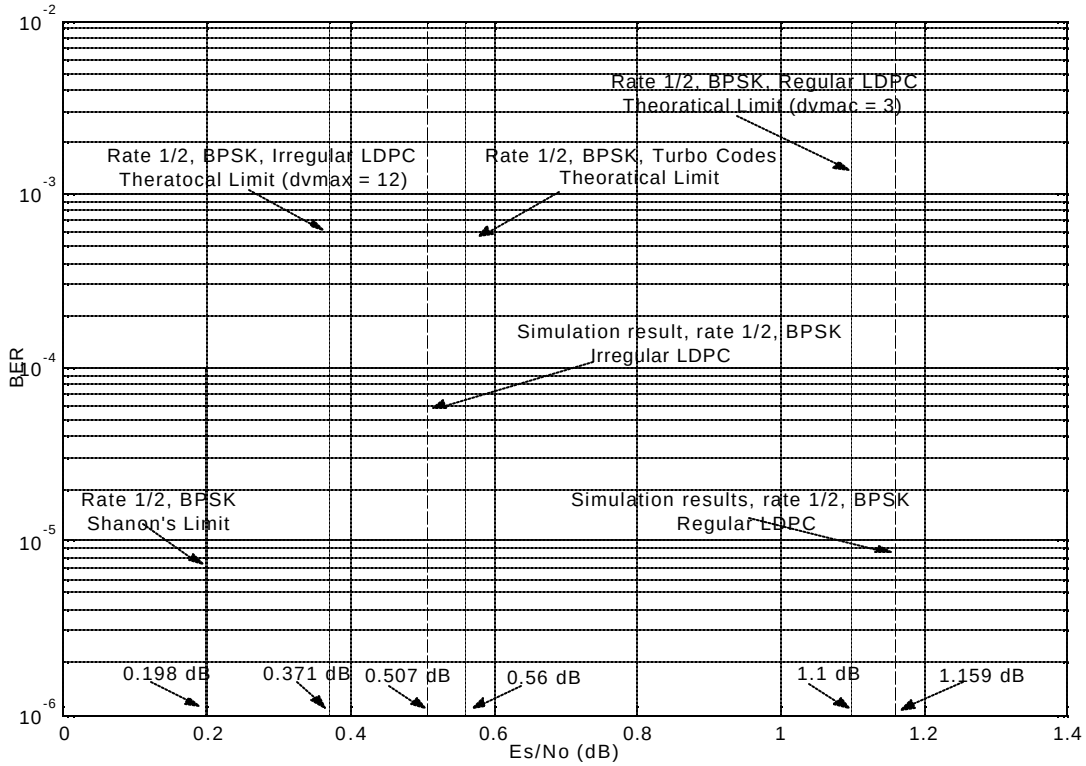

Fig. 27. Performance of LDPC codes (irregular and regular)

Also, intuitively for a better performance, variable nodes should have more message edges; allowing for an accurate judgment of the correct value of the bit whereas check nodes should have fewer edges; so that the information it send should be valuable. Since, the total number of edges is fixed, if check nodes has less (high) edges then variable nodes will have less (high). Irregular codes allow for the compromise in that the edges can vary. That is why irregular LDPC codes perform better than regular ones. It is also evident from the Fig. 28; an increase in the maximum number of edges, connected to variable node, results in improved performance. However, it shows diminishing returns as the block length is fixed at 256k bits. Increasing the block size will improve the performance. The results are presented in Table VIII.

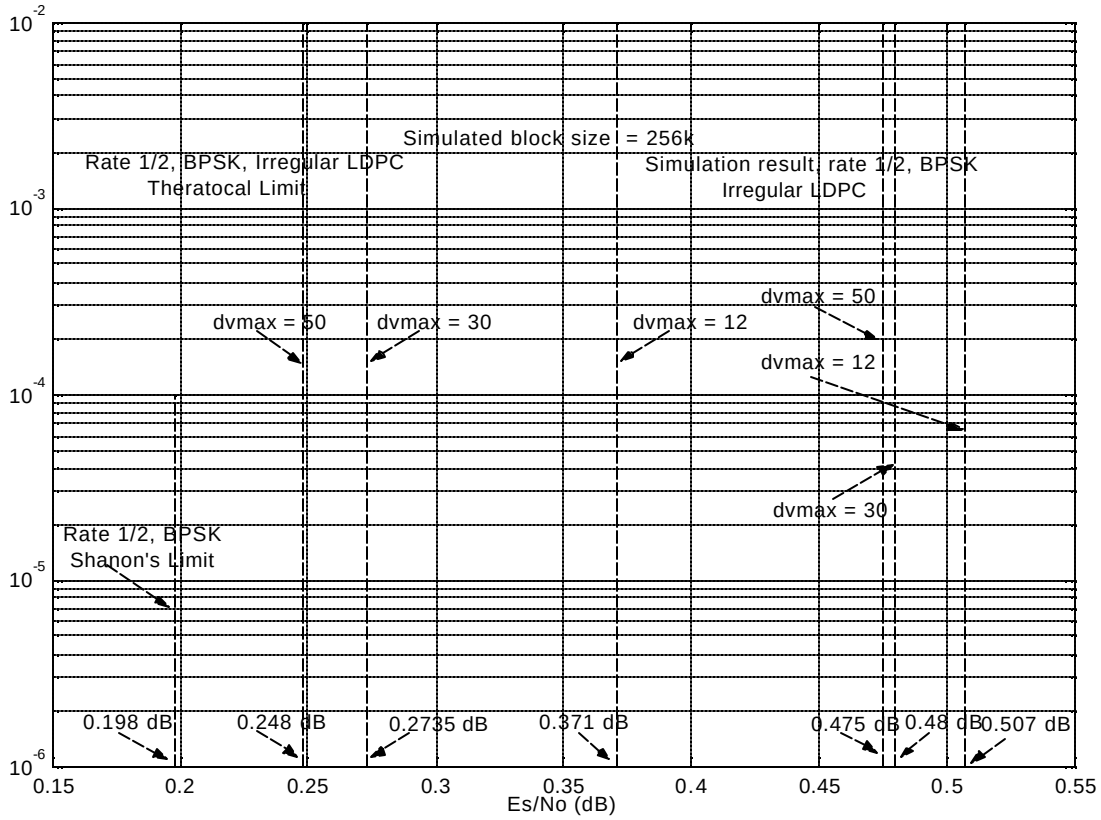

Fig. 28. Effect of dvmax on the performance of irregular LDPC codes

TABLE VIII

EFFECT OF *DVMAX* ON RATE 1/2

IRREGULAR LDPC CODE WITH 128K BLOCK SIZE

dvmax	Theoretical Limit Threshold (db)	Simulated (dB)	SNR-GAP (dB)	Gain over Turbo code (dB)
12	0.3710	0.507	0.502	0.053
30	0.2735	0.480	0.282	0.080
50	0.2480	0.475	0.277	0.085

4.3.3 LDPC Coded Modulation

As with the case of coded modulation with Turbo codes, similar techniques are developed for LDPC codes [41]-[46]. Following the approach of section 3.2.3, LDPC coder for QPSK signaling format is designed and applied to the JSCC framework. The results are shown in Fig. 29.

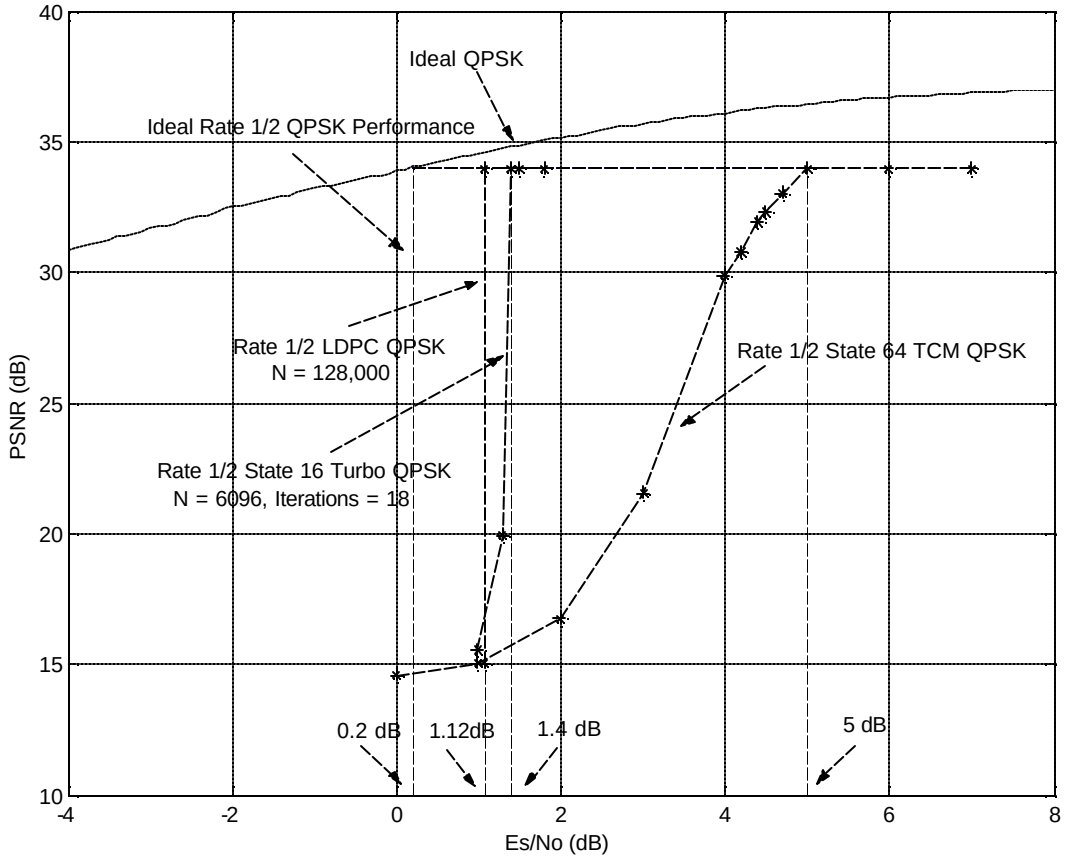

Fig. 29. Performance of rate 1/2 LDPC code with QPSK (dvmax = 50)

The LDPC system performs 0.27 dB and 3.87 dB better than the Turbo system and TCM system respectively for QPSK system. The overall performance achieved for the JSSC scheme with rate 1/2 code using various coding schemes (e.g. TCM, Turbo and LDPC codes) for QPSK modulation is presented in Table IX.

TABLE IX

GAIN ACHIEVED BY USING CHANNEL-CODING TECHNIQUES FOR RATE 1/2 CODE WITH QPSK SIGNALING

Channel Coding Scheme	Gain from Uncoded System (dB)	SNR-GAP (dB)
TCM	5.2	6.4
Turbo	8.8	1.2
LDPC (Irregular)	9.08	0.92

The results show that the new JSCC technique is optimal for bandwidth and power constrained channel and when used in conjunction with strong random coding techniques, it shows promising results and is quite near to the capacity-achieving SNR value of various channel signaling using this JSCC scheme. Similar result can be achieved by using turbo and LDPC codes with various rates and MPSK modulations.

CHAPTER V

CONCLUSION

In this thesis, a general framework is presented to determine the optimum JSCC scheme for embedded sources under a power and bandwidth constrained noisy channel. This framework also offers an additional degree of freedom, bandwidth constraint, with respect to the previously proposed UEP approaches. The framework is applied to progressive image coding transmission using constant envelope MPSK signaling (coded and uncoded) over the AWGN channel. The results show that the coded system performs on average 4 dB better than uncoded system. An adaptive MPSK-TCM system employing, a single encoder-decoder, is then presented for practical implementation of the proposed JSSC scheme. Finally, the performance of the scheme is investigated using capacity achieving codes like Turbo codes and LDPC codes. Results illustrate the fact that our framework performs close to the capacity-achieving SNR value of various channel signaling.

REFERENCES

[1] C. E. Shannon, "A Mathematical Theory of Communication", *Bell Systems Technical J.*, vol. 27, pp. 379-423 and 623-656, October 1948

[2] C. E. Shannon, "Coding Theorems for a Discrete Source with a Fidelity", *in Proc. IRE Nat. Conv. Rec.*, New York, NY, March 1959, vol. 7,pp.142-163

[3] P. G. Sherwood and K. Zeger, "Progressive Image Coding for Noisy Channels", *IEEE Signal Processing Letters*, vol.4, pp.189-191, July 1997

[4] A. Said and W. A. Pearlman, "A New, Fast, and Efficient Image Codec Based on Set Partitioning in Hierarchical Trees", *IEEE Trans. Circuits and Systems for Video Technology*, vol. 3, pp. 243-250, June 1996

[5] P. G. Sherwood and K. Zeger, "Error Protection for Progressive Image Transmission over Memoryless and Fading Channels", *IEEE Trans. Commun.*, vol. 46, no. 12, pp. 1555–1559, 1998

[6] G. Davis, J. Danskin, " Joint Source and Channel Coding for Image Transmission over Lossy Packet Networks", in *Proc. SPIE Conf. Wavelet Application of Digital Image XIX*, Denver, CO, August 1996, pp.376-387

[7] A. E. Mohr, R. Anand and K. Ramachandran, " Wireless Image Transmission using Multiple-Description Based Concatenation Codes", in *Proc. SPIC*, vol. 3974, January 2000, pp.300-311

[8] A. E. Mohr, E. A. Riskin and R. E. Ladner, "Unequal Loss Protection: Graceful Degradation of Image Quality over Packet Erasure Channels Through Forward Error Correction", *IEEE J. on Selected Areas in Commun.*, vol. 18, no. 7, pp. 819-828, December 2000

[9] M. Fossorier, Z. Xiong and K. Zeger, "Progressive Source Coding for a Power Constrained Gaussian Channel, " *IEEE Trans. Commun.*, vol.49, pp. 1301-1306, August 2001

[10] A. Alatan, M. Zhao and A. Akansu, "Unequal Error Protection of SPIHT Encoded Image Bit Streams," *IEEE J. Selected Areas in Commun.*, vol.18, pp.814-818, June 2000

[11] D. Mukherjee and S. Mitra," A Vector Set Partioning Noisy Channel Image Coder with Unequal Error Protection," *IEEE J. Selected Areas in Commun.*, vol.18, pp.829-840, June 2000

[12] V. Chand and N. Farvardin, "Progressive Transmission of Images over Memoryless Noisy Channels," *IEEE J. Selected Areas in Commun.*, vol.18, pp.829-840, June 2000

[13] B. Banister, B. Belzer and T. Fischer, "Robust Image Transmission Using JPEG2000 and Turbo Codes," *IEEE Signal Processing Letters*, vol. 9, pp. 117-119, April 2002

[14] G. Ungerboeck, "Channel Coding with Multilevel/Phase Signals", *IEEE Trans. Inform. Theory*, vol.28, pp.55-67, June 1982

[15] S. Benedetto, M. Mondin and G. Montorsi, "Performance Evaluation of Trellis-Coded Modulation Scheme", in *Proc. IEEE*, vol. 82, No. 6, June 1994

[16] S. Benedetto, M. A. Marsan, G. Albertengo and E. Giachin, "Combined Coding and Modulation: Theory and Applications", *IEEE Trans. Inform. Theory*, vol. 34, no. 2, March 1988

[17] A. J. Viterbi, J. K. Wolf, E. Zehavi and R. Padovani, "A Pragmatic Approach to Trellis Coded Modulation", *IEEE Commun. Magazine*, pp.11-99, July 1989

[18] J. K. Wolf and E. Zehavi, "P^2 Codes: Pragmatic Trellis Codes utilizing Punctured Convolutional Codes", *IEEE Commun. Magazine*, vol. 33, pp.94-99, February 1995

[19] C. Berrou and A. Glavieux," Near Optimum Error Correcting Coding and Decoding: Turbo Codes," *IEEE Trans. Commun.*, vol.44, pp.1261-1271, October 1996

[20] D. MacKay and R. Neal, "Near Shannon Limit Performance of Low Density Parity Check Codes," *Electronic Letter*, vol.33, pp.457-458, March 1997

[21] R. Gallager, "Low Density Parity Check Codes", PhD dissertation, Dept. of Electrical Eng., MIT, Cambridge, MA, June 1963

[22] J. M. Shapiro, "Embedded Image Coding using Zero-Trees of Wavelet Coefficients," *IEEE Trans. Signal Processing*, vol. 41, no. 12, p. 3445-3462, 1993

[23] J. G. Proakis, *Digital Communications* (Fourth Edition), New York: McGraw-Hill, 2001

[24] S. B. Wicker, *Error Control Coding Systems for Digital Communication and Storage*, Englewood Cliffs, NJ: Prentice-Hall, 1995

[25] J. B. Chai, G. C. Clark and J. M. Geist, "Punctured Convolutional Codes of Rate (n-1)/n and Simplified Maximum Likelihood Decoding," *IEEE Trans. on Inform. Theory*, vol. 25, pp. 97-100, January 1979

[26] J. Kim and G. J. Pottie, " On Punctured Trellis-Coded Modulation", *IEEE Trans. Inform. Theory*, vol. 42, no. 2, pp. 627-636, March 1996

[27] N.S. Raja, Z. Xiong and M. Fossorier, "Combined Source-Channel Coding for a Power and Bandwidth Constrained Noisy Channel with Application to Progressive Image Transmission", in *Proc. 36th Asilomar Conf. on Signals, Systems and Computers*, Pacific Grove, CA, November 2002

[28] C. Schlegel, *Trellis Coding*, Englewood Cliffs, NJ: IEEE Press, 1997

[29] L. Bahl, J. Cocke, F. Jelinek and J. Raviv, "Optimal Decoding of Linear Codes for Minimizing Symbol Error Rate," *IEEE Trans. Inform. Theory*, vol. 20, pp. 284-287, March 1974

[30] C. Fragouli and R. D. Wesel, "Turbo-Encoder Design for Symbol-Interleaved Parallel Concatenated Trellis-Coded Modulation", *IEEE Trans. Commun.*, vol. 49, pp. 425-435, March 2001

[31] P. Robertson and T. Wores, "Bandwidth-Efficient Turbo Trellis-Coded Modulation Using Punctured Component Codes," *IEEE J. Selected Areas in Commun.*, vol.16, pp.206-218, February 1998

[32] D. Divsalar and F. Pollara, "On the Design of Turbo Codes", *TDA Progress Report* 42-123, pp.99-121, Jet Prop. Lab., Pasadena, CA, November 1995

[33] D. Divsalar and F. Pollara, "Turbo Codes for Deep Space Communication", *TDA Progress Report* 42-123, pp.29-39, Jet Prop. Lab., Pasadena, CA, February 1995

[34] C. Berrou and M. Jezequel, "Non-Binary Convolutional Codes for Turbo Coding", *Electronics Letters*, vol.35, no.1, pp. 39-40, January 1999

[35] P. Robertson and T. Wores, "Coded Modulation Scheme Employing Turbo Codes", *Electronics Letters*, vol. 31, no. 18, pp. 1546-1547, August 1995

[36] C. Berrou, M. Jezequel, C. Douillard and S. Kerouedan, "The Advantage of Non-Binary Turbo Codes", in *Proc. IEEE Inform. Technology Workshop*, Caines, Australia, September 2001, pp.61-63

[37] S. L. Goff, A. Glavieux and C. Berrou, " Turbo-Codes and High Spectral Efficiency Modulation", in *Proc. IEEE Conf. on Comm.*, New Orleans, LA, May 1994, vol. 3, pp. 1255-1259

[38] D. J. C. MacKay, "Good Error-Correcting Codes Based on Very Sparse Matrices," *IEEE Trans. Inform. Theory*, vol. 45, pp.399-431, March 1999

[39] T. J. Richardson and R. L. Urbanke, "The Capacity of Low-Density Parity-Check Codes Under Message-Passing Decoding," *IEEE Trans. Inform. Theory*, vol. 47, no. 1, pp. 599-618, February 2001

[40] T. J. Richardson, and R. L. Urbanke, "Efficient Encoding of Low-Density Parity-Check Codes," *IEEE Trans. Inform. Theory*, vol. 47, no.1, pp. 638-656, February 2001

[41] T. J. Richardson, M. A. Shokrollahi and R. L. Urbanke, "Design of Capacity-Approaching Irregular Low-Density Parity-Check Codes," *IEEE Trans. Inform. Theory*, vol. 47, no. 1, pp. 619-637, February 2001

[42] R. Narayanaswami, "Coded Modulation with Low-Density Parity-Check Codes", M.S. thesis, Dept. of Electrical Eng., Texas A&M University, College Station, TX, June 2001

[43] J. Hou, P. H. Siegel, L. B. Milstein and H. D. Pfister, "Capacity-Approaching Bandwidth-Efficient Coded Modulation Scheme Based on Low-Density Parity-Check Codes", *IEEE Trans. Inform. Theory*, vol. 49, no. 9, pp.2141-2154, September 2003

[44] J. Hou, P. H. Siegel, L. B. Milstein and H. D. Pfister, "Multilevel Coding with Low-Density Parity-Check Codes", in *Proc. IEEE Global Telecommun. Conf.*, San Antonio, TX, November 2001, pp.1016-1020

[45] X. Li, J. A. Ritcey, "Bit-Interleaved Coded Modulation with Iterative Decoding", *IEEE Commun. Lett.* , vol. 1, pp. 169-171, November 1997

[46] K.R. Narayanan, J. Li, "Bandwidth Efficient Low-Density Parity-Check Coding using Multilevel Coding and Iterative Multi-Stage Decoding", in *Proc. 2nd Turbo Sym. Turbo Codes and Related Topics*, Brest, France, July 2000, pp.165-168

VITA

Nouman Saeed Raja was born in Rawalpindi, Pakistan, on October 4th, 1979. In May 2001, he graduated from Ghulam Ishaq Khan Institute of Engineering Sciences and Technology, Topi, Pakistan with a Bachelor of Science degree in electronics engineering. He was on the Dean's honor role throughout his undergraduate studies. In August 2001, he was admitted to Texas A&M University, College Station, Texas and graduated in December 2003 with a Master of Science degree in electrical engineering. He received a departmental scholarship from the Department of Electrical Engineering from August 2001-2003. He was employed by the department as a Teaching Assistant for the year 2002.

Mr. Raja can be reached at this address:

Nouman Saeed Raja
37/3, Al-Nazar, St. No. 2
New Lalazar, Rawalpindi 46000
Pakistan